

BB



Michigan State University

MSUCL 922
SW 9422

National Superconducting Cyclotron Laboratory

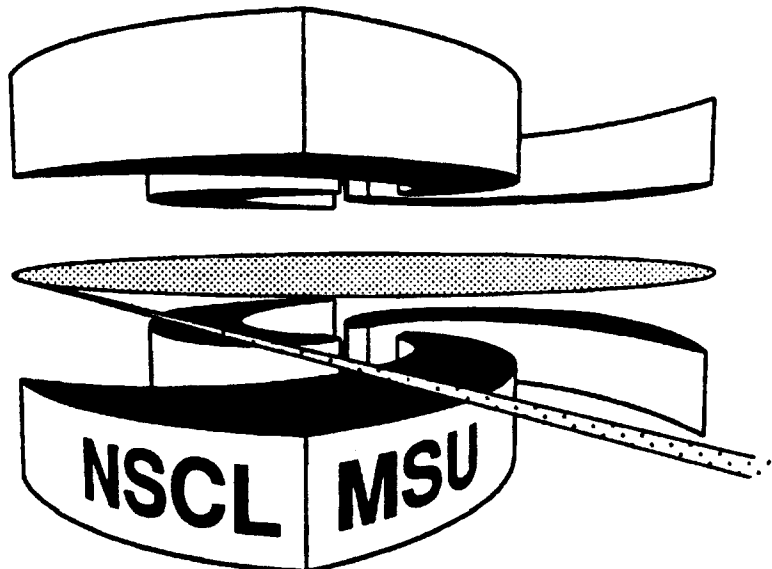
CERN LIBRARIES, GENEVA



P00023428

MEASUREMENT OF TEMPERATURE IN NUCLEAR REACTIONS

**DAVID MORRISSEY, WALTER BENENSON,
and WILLIAM A. FRIEDMAN**



MSUCL-922

FEBRUARY 1994

MEASUREMENT OF TEMPERATURE IN NUCLEAR REACTIONS

David J. Morrissey

National Superconducting Cyclotron Laboratory and
Department of Chemistry,
Michigan State University, East Lansing, MI 48824-1321

Walter Benenson

National Superconducting Cyclotron Laboratory and
Department of Physics and Astronomy,
Michigan State University, East Lansing, MI 48824-1321

William A. Friedman

Department of Physics
University of Wisconsin, Madison, WI 53706

MEASUREMENT OF TEMPERATURE IN NUCLEAR REACTIONS

David J. Morrissey

National Superconducting Cyclotron Laboratory and
Department of Chemistry,
Michigan State University, East Lansing, MI 48824-1321

Walter Benenson

National Superconducting Cyclotron Laboratory and
Department of Physics and Astronomy,
Michigan State University, East Lansing, MI 48824-1321

William A. Friedman

Department of Physics,
University of Wisconsin, Madison, Wisconsin 53706

Short running title: **Nuclear Temperatures**

Key words: *Heavy Ion Reactions, Temperature, Entropy, Equilibrium, Statistical Emission, Evaporation Spectra, Complex Fragment Emission, Excited State Populations, Unbound Nuclear States, Sequential Feeding*

Mailing address for proofs:

D.J. Morrissey
National Superconducting Cyclotron Laboratory
Michigan State University
East Lansing, MI 48824-1321
Phone: (517) 355 9554; Fax: (517) 353 5967

Contents

1	Introduction	4
1.1	Basic Definition of Nuclear Temperature	6
1.2	Applicability of the Basic Definition	8
2	General Procedures for Temperature Measurement	10
2.1	Introductory Remarks	10
2.2	Connection with the Fundamental Definition	11
2.3	Treatment of Densities of States	14
3	Spectra of Emitted Particles	19
3.1	General Form of Spectra	19
3.2	Sudden Disintegration	21
3.3	Corrections to the Spectra	22
3.4	Representative Measurements	25
4	Relative Yields of Different Species	27
4.1	Total Yields	27
4.2	Yields of Bound Excited States	29
4.3	Measurements of Bound States	31
4.4	Yields of Unbound States	35

4.5	Measurements of Unbound States	36
5	Conclusions	41
6	Acknowledgements	42

1 Introduction

Bridges between different fields of physics have always provided fruitful insight into the exploration of new phenomena. The link between microscopic atomic nuclear systems and complex macroscopic systems is one such bridge. For the latter, thermodynamics and statistical mechanics have been effective tools. Thus, it was reasonable to develop thermodynamic concepts, such as temperature and entropy, for nuclear systems. This development permits a discussion of new nuclear phenomena in a language which was more often used with macroscopic systems.

One of the most intriguing phenomena observed in macroscopic systems is that of a phase transition. Analogous phenomena have been sought in nuclear systems, and today two specific areas are receiving a great deal of attention. One involves the loss of stability by excited nuclear systems at intermediate energies under certain conditions of temperature and density which may lead to the disassembly of the nucleus into massive fragments. The second, at much higher energies, concerns the transition from hadrons to quarks, and the possibility of observing new phenomena in quark matter, which is totally unexplored. Evidence for both phase transitions comes, in part, from the measurement of temperature in hot systems which are produced in heavy ion collisions.

The concept of a nuclear temperature was introduced very early in the field in the pioneering work of Bethe(1) and Weisskopf(2). That work was intimately connected with the exploration of the compound nucleus created in the bombarding nuclear targets by light projectiles. The early work demonstrated the usefulness of the concept of temperature in a nuclear context. The subject of temperature has been recently reexamined in the context of reactions at higher energy, and those involving collisions between heavy ions, for examples see the recent reviews (3, 4) and references therein. Here questions of its validity have been raised, and new methods have been used for its measurement. In this review we will examine some of these questions and problems, and discuss the recent methods which have been applied to the measurement of temperature. We will, however, not attempt to survey the entire history and development of the broad topic of temperature.

The concept of equilibrium is closely linked to the idea of nuclear temperature. A fundamental definition of equilibrium is the equipartition of the available energy among all of the degrees of freedom, and evidence for this partition of energy is available in the broad range of products that are emitted by excited nuclear systems. This aspect of nuclear behavior has been examined within the framework of the “statistical model,” and a discussion of the many facets of this model has already been presented by Stokstad(5).

Before considering the detailed topic of the ‘measurement’ of nuclear temperature, we will define this temperature carefully, and examine its validity in the context of nuclear reactions. This will be discussed in the next subsections. Subsequently, we will outline the general classes of procedures which are currently being used to determine magnitude of temperature in the following sections. We will attempt to link these procedures closely to the fundamental definitions.

Over the years, three general classes of measurements have been used both to test for equilibrium and to evaluate the temperature: observation of a Maxwell-Boltzmann velocity spectrum for an individual particle (2), the relative yields of emitted particles (6), and the relative populations of internal states of emitted particles (7). For each general class of measurement we will discuss the formalism and features that complicate the extraction of information about temperature. In the following sections we also review specific recent measurements which have been performed and the results obtained in each case.

A survey of the literature shows that an enormous amount of effort has been devoted to studies of the $^{14}\text{N}+\text{Ag}$ system at $E/A=35$ MeV. As indicated in Table 1, the entire range of techniques that we will describe has been applied to this system with somewhat discordant results. The reasons for this focussed effort are largely historical stemming from the fact that the initial application of a new technique based on excited state populations showed a serious discrepancy among the techniques for this particular system. We will use this system as a thread to combine and focus our discussion.

1.1 Basic Definition of Nuclear Temperature

In collisions between large nuclear systems, collective translational kinetic energy can be deposited into other modes, predominantly the microscopic degrees of freedom of the total system. One area of nuclear research seeks to explore this process and the subsequent role the deposition plays in determining the type and behavior of the final-state particles produced in the collision. Full damping, with the attainment of equilibration, represents a limit to this process, and nuclear temperature is one of the natural variables used to characterize systems that have reached this limit.

At the start, it is essential to emphasize the difference between excitation energy and temperature. A system which is highly excited is often referred to as being “thermally hot”. This expression, however, is not refined enough to make the important distinction between these two quantities. An individual nucleus is one of nature’s most perfect examples of an isolated system. Since the nuclear force has a very short range, a nucleus normally does not share its excitation energy with its external environment. For this reason some of the classical concepts of temperature which are associated with external heat reservoirs are not applicable to nuclear systems. In addition, a whole ensemble of nuclear systems are created in nuclear reactions, and it is the average behavior of this ensemble to which the concept of temperature is applied. Thus the ensemble average over isolated systems which is envisioned in statistic mechanics may be relevant to an assemblage of nuclei excited in a reaction.

The concept of temperature has been defined with great precision in classical statistical mechanics, and we shall apply this definition to nuclear systems. With this approach we can easily make the distinction between excitation energy and temperature.

We now turn briefly to general statistical mechanics(8) in order to review some fundamental quantities that are used to define temperature for isolated systems. One of these is the number of states near a given total energy. For our discussion let $\Gamma(E, N)$ specify the number of states of a given system, with fixed volume and particle number N , which lie in the vicinity (ΔE) of energy E . This function is, of course, directly proportional to the density of states at energy E , represented by $\rho(E, N)$, such that

$$\Gamma(E, N) = \rho(E, N) \times \Delta E. \quad (1)$$

It is also convenient to introduce the entropy of the system, $S(E, N)$, by,

$$S(E, N) = \ln\Gamma(E, N) = \ln\rho(E, N) + \ln\Delta E \quad (2).$$

With these quantities, the definition of temperature provided by statistical mechanics is

$$\frac{1}{T} = \frac{\partial S(E, N)}{\partial E} = \frac{\partial \ln\rho(E, N)}{\partial E}, \quad (3)$$

where we have taken ΔE to be independent of E . This definition is as applicable to a nuclear system as it is to any other isolated system. The only difference is that the appropriate density of states, $\rho(E, N)$, must be used. A detailed discussion of this density will be made after an exposition of the general application of this definition.

1.2 *Applicability of the Basic Definition*

While the formal definition of temperature is simple, the relevance of the concept and its measurability depend on further requirements which, in most realistic nuclear cases, may only be approximately met. The excitation of an isolated system may be characterized by an energy, but statistical mechanics shows that two additional major features, i.e., the degree of equilibration and the specific density of states, must be known to characterize an ensemble of systems with a temperature.

The most critical of these requirements is that the ensemble be in full statistical equilibrium. By this we mean that each of the states included in $\rho(E, N)$ is populated with equal probability. In this case it is appropriate to characterize the ensemble by a *temperature*, and then and only then will it be possible to measure the value of that temperature. For highly excited nuclear systems, the requirement of full equilibrium may be difficult to achieve in practice. As the excitation energy increases, the lifetime of the system becomes dramatically shorter, thus reducing the likelihood that all the

states are populated with equal probability. It is difficult to know, *a priori*, the degree to which equilibrium is achieved because the dynamics governing the evolution of the nuclear system is imperfectly known.

Nonetheless, in order to explore the question of equilibrium it is instructive to assume that the population of states is sufficiently complete to permit the use of the concept of temperature. Operationally, the predictions of statistical equilibrium for specific nuclear systems are often compared to experimentally observed distributions as a test for thermal equilibrium. If the system is truly in equilibrium, then a variety of consequences follow. This permits one to look for several signatures of equilibrium as confirmation that the condition is met. In particular, different methods for measuring the temperature should all provide the same result. As we shall see, the hoped for agreement among temperature measurements is not always found. The lack of agreement argues against the existence of thermal equilibration. On the other hand, it may also have other explanations since the measurements can be influenced by aspects other than equilibrium. We shall discuss some of these features below.

Just as a determination of temperature requires an assumption about the degree of equilibrium, it also requires additional assumptions about the density of states. This aspect of nuclear systems can not be precisely determined from first principles. We will devote a section below to a detailed comment on the range of approaches taken to approximate the density of states, especially of nuclei at high excitation energies.

2 General Procedures for Temperature Measurement

2.1 Introductory Remarks

The basic definition of temperature provides a framework for a discussion of the general procedures used to measure its value. For the purposes of the discussion we will assume that the conditions of equilibrium are sufficiently met and that the necessary level densities are known. In addition, we will assume that the excitation energy is known or, at least, that it has a definite value. This last requirement may be difficult to fulfill in realistic situations as fluctuations in the value of the energy deposited during each nuclear collision may be quite large, particularly when several reaction mechanisms contribute to the emission of a given product. For example, in one case a systematically varying portion of the colliding system becomes strongly involved in the collision (incomplete fusion), in another case a fraction of the particles leave the system before equilibrium is achieved and remove various amounts of energy (pre-equilibrium particle emission). Uncertainties introduced by processes like these can introduce wide variations into the value of the excitation energy obtained for a given target, projectile, and bombarding energy combination. It is essential to have a well characterized system in order to extract meaningful temperatures. This requirement, in turn, has spurred efforts to use coincidence techniques and various reaction filters to select events that are similar in excitation energy as a prelude to any attempt to measure temperature.

In classical measurements of the temperature of macroscopic systems, small external test-systems are generally brought into thermal contact with the system of interest. The test-systems are small and do not significantly perturb the macroscopic system. The response of these test-systems, which is assumed to be standardized

and well understood, is observed to provide the temperature measurement. Such a procedure is clearly not possible for nuclear systems, which interact weakly with their environment. For nuclear systems information is conveyed not through interaction with an external test-system, but rather through the emission of small portions of the system itself. The measurement of *temperature* then relies on the assumption that these small portions have shared in the equilibrium and density of states and are characteristic of system as a whole.

The experimental procedures for temperature determination which we outline next involve the examination of three aspects of the emitted particles: their kinetic energy spectra, their relative number, and their excited state populations. We will show that, in an ideal situation, each of these aspects can provide measurements of the same quantity. Under realistic situations, however, each may be influenced in different ways by the prevailing nuclear conditions. For this reason it is important to apply as many different techniques and variations as possible to determine a nuclear temperature.

2.2 Connection with the Fundamental Definition

Let us consider the fundamental features of the distributions of emitted particles that permit the determination of temperature for the ideal case. We consider the case in which a portion of the system is emitted and leaves behind a residue which we call the “daughter.” If equilibrium has been achieved prior to emission, then the energy will be shared between the emitted portion and the daughter. If the energy and number of particles in the primary system is large enough, and the emitted energy and emitted portion are small enough, then the daughter can serve the role of a heat bath in classical thermal dynamics. Following the procedures of standard statistical mechanics, the relative weight for each final state of the emitted system is given by

the number of states available to the daughter. Specifically, let us characterize the small emitted system by a mass number, n , and an energy, ϵ , from an initial system with a mass number, A , and a total energy, E . The emitted energy, ϵ , contains the translational kinetic energy, ϵ_k , the separation energy, ϵ_s , and any internal energy ϵ_r , all associated with the small emitted portion:

$$\epsilon = \epsilon_k + \epsilon_s + \epsilon_r. \quad (4)$$

It follows from counting states that the general expression for the relative probability, $P(\epsilon, n)$, for obtaining an emitted portion with n and ϵ is given by

$$P(\epsilon, n) \propto \Gamma(\epsilon, n) \times \Gamma(E - \epsilon, N - n), \quad (5)$$

where $\Gamma(E, N)$ is the number of states in the vicinity of energy E for a system of mass number N , the first factor being contributed by the emitted system while the second being contributed by the daughter. The numbers of states is given by the general functions introduced in Eq.1. We need to obtain the integrated emission rates which produce the total yields measured in nuclear reactions. It is from these yields that temperature is to be determined.

Various models have been proposed to relate the rate of emission to $P(\epsilon, n)$. One of the best known models for the emission rate, used for the sequential emission of nuclear fragments, is based on detailed-balance and was first proposed by Weisskopf (2). This model provides that

$$\frac{d^2 N}{dt d\epsilon_k} \propto \frac{(\epsilon_k)^{\frac{1}{2}} \sigma}{\Gamma(E, A)} \times P(\epsilon, n), \quad (6)$$

where $d^2 N/dt d\epsilon_k$ is the rate for emission of a specific portion of size n and translational kinetic energy near ϵ_k from an original system of size A and energy E . The factor σ provides the cross section for the inverse reaction, i.e., the absorption of the

emitted portion by the (suitably excited) daughter. Such cross sections are essentially unknown and, therefore, are taken from inverse reactions on ground state nuclei.

Substituting the probability given in Eq.5 for that in the rate of emission, Eq.6, one finds the ratio

$$\frac{\Gamma(E - \epsilon, A - n)}{\Gamma(E, A)} = \exp(-(S(E, A) - S(E - \epsilon, A - n))), \quad (7)$$

where the exponential of the entropies, defined in Eq.2, has been inserted for the level densities. For small values of ϵ/E and n/A this ratio can be approximated by a Taylor series expansion, some of whose important terms are given by,

$$\exp(-\epsilon \left(\frac{\partial S}{\partial E} \right)_A) + \dots = \exp(-\epsilon/T\dots). \quad (8)$$

Thus, the original Weisskopf emission rate contains, through this factor, the explicit influence of temperature following directly from the fundamental definition of statistical mechanics that $1/T = (\partial S/\partial E)_N$.

The different methods developed over the years to determine the nuclear temperature all follow from Eq.8 but make use of different terms in ϵ as indicated in Eq.4. Note that the relative probabilities of *like* emitted fragments will have many factors in common that will drop out of any ratio. Anticipating later discussion, the form for the kinetic energy spectrum of a single fragment incorporates substantial cancellations (but is the most sensitive to temporal integration), whereas the relative probabilities of *unlike* emitted fragments have substantially unknown factors. Significant cancellation and a lesser degree of sensitivity to temporal evolution is found for the emission of excited states of a single fragment (but sequential decay of other emitted species can pose problems). Before continuing with the application of these ideas to experimental situations, a discussion of some of the intricacies of the nuclear level densities is presented in the following section.

2.3 Treatment of Densities of States

We have noted that the crucial link between excitation energy and temperature is the density of many-body states of the system during decay. We should note that the density of states of normal nuclei is only known at low excitation energies. At this point it is useful to consider how to evaluate the density of states or equivalently the entropy.

Up to now we have not distinguished nuclear systems and macroscopic systems on the basis of their size. There is, however, at least one important difference between the two and that is the way the entropy $S(E)$ is commonly evaluated. In statistical mechanics one considers different physical situations (ensembles) for evaluating thermodynamic quantities: fixed energy and particle number (microcanonical ensemble), fixed temperature and particle number (canonical ensemble), and fixed temperature and chemical potential (grand canonical ensemble). In the evaluation of thermodynamic quantities for macroscopic systems each of these approaches provides essentially the same result. Thus, the entropy may be evaluated by obtaining any of the following: $S_{\text{microcanonical}}$, $S_{\text{canonical}}$, or $S_{\text{grandcanonical}}$. This is not the case for the smaller nuclear systems because the only appropriate ensemble is the microcanonical ensemble used for isolated systems. The fundamental definition of nuclear temperature is thus

$$\frac{1}{T} = \frac{\partial S_{\text{microcanonical}}(E, N)}{\partial E} \quad (9)$$

and it is not correct to substitute an entropy obtained with a different ensemble into this expression.

A great deal of study has shown that the level densities of nuclei at low excitation energies have a energy dependence similar in form to that of a Fermi gas. Standard

procedures permit the evaluation of the entropy of a Fermi gas under the conditions of a *grand canonical* ensemble. For low excitation energies, E^* , the entropy is:

$$S_{\text{grandcanonical}}(E^*, N) = 2(aE^*)^{\frac{1}{2}}, \quad (10)$$

where a is a constant proportional both to the number of particles and to the density of the single-particle levels of the Fermi gas at the Fermi energy, ϵ_f . If $S_{\text{grandcanonical}}$ is used to replace $S_{\text{microcanonical}}$ in Eq.9, one obtains $T = (E/a)^{\frac{1}{2}}$ as the link between temperature and excitation energy. This result would be appropriate for macroscopic systems, but it must be modified for isolated nuclear systems. For small systems

$$S_{\text{microcanonical}} = S_{\text{grandcanonical}} + \Delta S, \quad (11)$$

where ΔS becomes vanishingly small compared to $S_{\text{grandcanonical}}$ as the number of particles or the excitation energy becomes large. An approximate expression for ΔS is available for a Fermi gas, where, at relatively low energy, one finds,

$$\Delta S \approx -\gamma \ln(E^*), \quad (12)$$

with γ being a number of the order of unity, ranging from 1 to 2 depending on whether isospin and angular momentum are explicitly considered in the labeling of the states. When the appropriate $S_{\text{microcanonical}}$ is used to evaluate the nuclear temperature one finds

$$\frac{1}{T} = \frac{\partial S_{\text{grandcanonical}}}{\partial E} + \frac{\partial \Delta S}{\partial E}. \quad (13)$$

For the moderately low energies this provides

$$\frac{1}{T} \approx (a/E^*)^{\frac{1}{2}} - (\gamma/E^*) \quad (14)$$

as the link between excitation energy and nuclear temperature. For large excitation energies, E^* , and large particle number the correction term proportional to γ vanishes.

Following the development of Fermi gases, it is customary to take the density of nuclear states to be

$$\rho(E^*) \propto \frac{a}{(aE^*)^\gamma} \exp(2(aE^*)^{\frac{1}{2}}). \quad (15)$$

The factor a here is called the level density parameter and is adjusted to correspond to level densities measured at low excitation energies (9, 10). These fits suggest that a is proportional to the mass of the nuclear system A , and it is further found that $a \approx A/8MeV^{-1}$. The level densities can be corrected for angular momentum by including pre-exponential statistical factors and subtracting the collective energy that is involved in rotation. The latter is often included with an effective moment-of-inertia, a parameter adjusted to match experimental spectra and yields.

In attempts to measure nuclear temperatures, the conventional procedure has been to find the best fit for a and the moment-of-inertia in the low energy regime. With these parameters the level density can be evaluated, and thus the link between excitation energy and temperature is established, e.g., (9, 10). If the excitation energy is well known, on the other hand, spectra and relative yields can be used to determine these parameters under the assumption of full equilibration.

At the higher excitation energies produced in collisions between massive nuclei with large relative energies, the level density of the many-body system is less known, and dynamics are important. In this regime there are at least three issues which involve the level density and should be examined. One would clearly expect some deviation from the form of the low energy Fermi gas expression given in Eq.14. This form is only valid in the limit of $T/\epsilon_f \rightarrow 0$, where ϵ_f is the value of the Fermi energy. The simplest approach is one that uses the generalization of Eq.13 which links E^* to T for a Fermi gas at any temperature. This approach was taken in Ref.(11) in which the effective Fermi energy is taken as a fitting parameter instead of the level density

parameter, a . Once ϵ_f is chosen, the extension to elevated energies follows from the ensemble averages of the Fermi gas. An extension of this approach is found in Ref. (12) in which the emitting system is assumed to expand. The change in density is expected to effect the Fermi energy, and this change is incorporated by the introduction of a simple density dependence for ϵ_f , so that it varies like $\rho^{\frac{2}{3}}$.

A second consideration which is made for the level density for highly excited nuclear systems is based on a more complete treatment of the quantum mechanics of the many-body system. In particular, one might expect energy and momentum dependencies in the mean-field which binds the particles. These effects can be treated by introducing an effective mass for the nucleons. That is, the effective mass, rather than the free value, is used when determining the energies of the particles in the gas. This has a subsequent effect on the level density as seen in the studies made by Shlomo, for example (13, 14, 15).

A third effect is associated with the short-lived nature of the excited single-particle states which are occupied by the nucleons. Various occupation schemes have been used to generate the many-body states which provide the level densities and entropies. The short lives of the single-particle states require that one decide *how* to count the contributions of individual nucleons to the overall level density. There have been two approaches to this problem both of which are based on the generation of a many-body level density from the occupation of independent single particle levels and follow, in principle, the development used for an ideal Fermi gas. One of these schemes is based on constructing two grand canonical partition functions: one representing a system composed of “nucleus plus vapor”, and the other composed of “vapor” alone. The difference between the free energies of these the two types of systems is assumed to supply a description of the hot nucleus alone.

This procedure, suggested by Tubbs and Koonin (16) and used in references (17) and (15), involves expressing the free energy of the hot system in terms of the difference between two partition functions, thus:

$$\ln Z(\beta, \mu; V_{nucleus}) - \ln Z(\beta, \mu; V_{vapor}). \quad (16)$$

Here $Z(\beta, \mu, V)$ represents the grand canonical partition function with a temperature $1/\beta$, a chemical potential μ and for a system of independent particles moving in the appropriate potential V .

In many cases it is assumed that the vapor particles move in no potential at all and V_{vapor} is set to zero. This subtraction procedure has been shown to generate a set of single-particle states, used for the many-body level density, which include the bound states and also the narrow resonances both below and above the coulomb-angular momentum barrier, but not the very broad, short-lived single-particle resonant states. Mustafa, *et al.* (18), recently examined a similar approach in which the effect on the many-body level density of rejecting single-particle levels which lie above the barriers in finite potentials was studied.

Both of these approaches reduce the level density at high excitation energies by eliminating contributions of high energy single-particle levels. In this excitation region the high-energy single-particle levels of a Fermi gas provide important contributions. These approaches are based on a consideration of the single-particle level densities and the life-times of these levels alone. The dynamical effects of collisions, which may also determine the life-time of the many-body emitting states, is beyond the scope of these models.

Finally for completeness, we wish to point out that in the formal reaction models such as the unified model of Feshbach or the R-matrix approach of Wigner, the

definition of compound “states” of an excited system is based on many-body states which satisfy specific boundary conditions. The density of such states is thus set by the imposed boundary conditions. In these formalisms, the “states” have discrete energies and acquire widths only through couplings to the open channels. The relationship between the density of these many-body compound nuclear states, and any reduced density suggested by the short-lived single-particle states, is not completely clear.

While there has been much theoretical effort in this interesting area, it is difficult at this time to find specific experimental evidence to suggest the greater validity of any one of the approaches described above. This is probably due to the fact that at high energies the influence of the level density is diluted by a wide range of other phenomena which contribute to the experimental spectra.

3 Spectra of Emitted Particles

3.1 *General Form of Spectra*

We first consider the details of the method of measurement of nuclear temperatures through the spectra of emitted particles. In this procedure one examines the relative yield of a specific single type of emitted particle at different values of kinetic energy, ϵ_k . Alternatively, the kinetic energy of the recoil can be measured but this is technically more difficult and less sensitive. From the discussion leading to Eq.8, the influence of the temperature on kinetic energy spectra would be expected to come through a factor of $\exp(-\epsilon_k/T)$ where ϵ_k is the kinetic energy. In addition, there will be a dependence on the kinetic energy in the $\Gamma(\epsilon, n)$ factor that is contained in $P(\epsilon, n)$, and another in the flux factor, $(\epsilon_k)^{\frac{1}{2}}$, from detailed-balance. The resulting expression

for the emission rate has the form:

$$\frac{dN^2}{dt d\epsilon_k} \propto (\epsilon_k - V_C) \exp(-\epsilon_k/T) \quad (17)$$

where V_C represents the Coulomb potential, which is necessary to include when considering emission of charged particles. Neutron spectra have long been used as sensitive probes of the nuclear temperature due to their copious emission and lack of Coulomb effects.

Without further consideration, one might expect that the observed spectra could be compared with the emission rate (Eq.17) to reveal the temperature. For example, the spectra of neutrons emitted from bismuth and tantalum compound nuclei are shown in Fig. 1. These data, from relatively simple neutron induced reactions, indicated the importance of sequential emission (19, 20). Such comparisons were made in the earliest work on single neutron emission that formed the basis of compound nuclear theory (6, 9, 10, 5) and have been applied to a wide range of nuclear reactions [cf., e.g., (21, 22, 23, 24, 25, 26, 27, 28, 29)]. The apparent simplicity is attractive, particularly the systematic variation with bombarding energy in the intermediate energy regime which has been extracted by Westfall, *et al.* (22) shown in Fig. 2.

However, such an application of this expression to complex nuclear reactions is too simple for several reasons which we will now elaborate. First, one must establish that a given species comes primarily from one emission process, in this case thermal evaporation. Then the expression in Eq.17 is for an *instantaneous* rate of emission. To obtain the measured spectrum, $dN/d\epsilon_k$, one must integrate over the time involved in the process. In the case of single-chance neutron emission from a (weakly) excited compound nucleus, the time integration does not change the overall dependence. However, when the emission of a given particle can occur over a range of times (with varying excitations) it will also occur over a range of temperatures T . Thus,

the observed spectra will be a convolution over these temperatures ranging from the highest, at the beginning of the emission process, down to the lowest, at the end. One would expect the highest energy part of the spectra (usually the smallest part of the differential cross section) to be dominated by the highest temperatures. Attempts have recently been made to use reaction filters to observe ‘first chance’ emission of particles (30, 31), and clearly these effects are present. Furthermore, since V_C as well as the temperature is expected to vary with emission time, the actual convolved spectra may appear quite different from Eq.17 (32). Only for the special case in which the emission occurs under a narrow range of conditions can a simple connection between temperature and the spectra be made through the use of Eq.17. Models which properly describe the temporal evolution or cooling during the emission process will have the best chance to describe the measured spectra. Such models have been available for a long time for statistical evaporation from compound nuclei [e.g., (33, 34, 35, 11)], preequilibrium emission [e.g., (36)] and binary decay [e.g., (37)] but are not used for ‘moving sources’ because sudden disintegration is invoked, as is discussed below.

3.2 Sudden Disintegration

It should be said that another scenario for the emission process, that of a sudden disintegration of the source into the observed fragments has been invoked to justify using the simple expressions above. Here, one is not faced with the question of evolution of the temperature variation inherent in a chain of successive decays. Rather, one assumes a single “freeze-out” condition. If the source that suddenly disintegrates was in equilibrium, the production cross section is determined by the probability $P(\epsilon, n)$ of Eq.5. Once more the spectra for a specific type of emerging particle is determined

by $\exp(-\epsilon_k/T)$ where T has the same definition as at given in Eq.8, and it reflects the fundamental definition from statistical mechanics. In this case the pre-factor, which multiplies the exponential in the spectra has a different power since one does not have the influence of the flux factor present in the sequential emission scenario. Furthermore, the Coulomb energy for each emerging fragment depends on the number and positions of all of the other fragments. This introduces more fluctuations in the spectra. In addition, one expects to have some of the same collective kinematic effects in the data discussed below. These include, in particular, the effects of angular momentum and fluctuations in the velocities of the source. Because a fragment can emerge from any location in the source, rather than from the surface alone, there will be additional fluctuations associated with the point of emission if any collective expansion is present.

It should be clear that there is a startling number of prerequisites for a nuclear system to meet to be an unambiguous test system for the determination of temperature. There must be a given amount of excitation energy deposited into the nuclear system, and that energy must be fully equilibrated among the microscopic degrees of freedom. Then the temperature can be defined by the fundamental definition of statistical mechanics, and also the level density, or instantaneous level density, of the source system must be known. The above conditions can only be met in an intermediate energy heavy ion collision only if the other dynamic aspects of the reaction are well understood. This is the basic task of the field of heavy ion reactions.

3.3 Corrections to the Spectra

The form of the spectral distributions, whether the emission is sequential or sudden, is also influenced by collective dynamical effects, some of which have been know for

some time. Three effects are of particular relevance in heavy-ion induced reactions: collective rotation, translational motion, and collective expansion of the source. Each of these can effect the spectral shape in ways that are similar to changing the temperature. The first of these, angular momentum, may be directly incorporated into the equilibrium description of the emission process by including angular momentum among the labels of the microscopic states for both the emitted system and the daughter system (38, 39). The effect of this additional labeling consists of a modification of the expected energy spectra of the emitted particles. In particular, particles which are emitted with high angular momentum but low temperatures display spectra which are not dissimilar from those of higher temperatures (40) and low angular momentum. Thus, if one is to learn about the temperature from spectra one must correct for the contribution from rotational motion. Only in a few 'moving source' calculations has such a correction been attempted, partially due to the lack of information on the conversion of orbital motion into intrinsic angular momentum in these collisions. A formula that includes the average source angular momentum can be found in Ref. (41).

Translational motion of the source also has a strong influence on the spectra which requires disentanglement if one is looking for information about the temperature of a system. The most straightforward effect to extract is the mean motion of the emitter. This has been dealt with phenomenologically by finding the source velocity or frame in which the spectra appear essentially isotropic. For systems in which angular momentum is an important feature, the azimuthal dependence with respect to the reaction frame is still not expected to vanish. More difficult to separate from thermal information are fluctuations about the mean velocity of the source. These fluctuations can also produce spectra which appear to show high temperatures. There are two

main origins for these velocity fluctuations. One is associated the early stages of the reaction during which incomplete momentum transfer can provide a distribution of source velocities. The second is associated with the temporal evolution of the source itself. Each emission is attended by a recoil of the source. The accumulation of these recoils introduces fluctuations in the source velocity which can influence the spectra. In particular, it can broaden the width of the peak in the spectra. Since both types of collective velocity fluctuations will boost the velocity from the emission frame to the laboratory frame, both will have an effect on the particle energy which increases with mass. In most practical applications three moving sources each with a single velocity and temperature are combined to fit the observed spectra. Depending on the degree of coverage of the angular distribution, the parameters are formally overdetermined but they are not orthogonal, and correlated variations are possible. Examples of early comprehensive data can be found in Refs. (23) and (24).

The last of the collective motions which we will consider is that of source expansion, or the radial motion of the material of the source. This effect has been considered as 'blast waves' (42) and also simple expansion (43). Here again one is faced with a boost of the velocity of the emitted system in the laboratory frame, and once more the effect increases with increasing mass of the emitted system observed. In Eq.17, above, the effect of the Coulomb acceleration following emission is treated by the strength the Coulomb force between the source and the emitted system. In the cases which involve high rates of emission, there is also a probability for a more complicated Coulomb interaction which can arise when three or more subsystems interact in the final state through their relative Coulomb fields. This effect is hard to estimate and requires a detailed model of the decay.

In summary, the temperature of the emitting system does act as the underlying

determinant of the spectra for each type of emitted particle, when the source is fully equilibrated. But a range of temperatures can be present for sequential emission chains, and these are not often treated in simple analyses. On the other hand, the spectra blend this information with several collective kinematic features each of which must be understood on its own before one attempts to extract the information on temperature. It should be noted, however, that it is in the high-energy tails of the spectra that information about the highest temperatures of the process is most readily available. Therefore, only at the lowest excitation energies is the procedure for extracting temperatures from the spectra straight forward. When light projectiles are used, angular momentum is not an important factor. At low energies, the fusion process is complete, there are no fluctuations in the excitation energy, and the transfer of momentum is complete. Also at low energies, pre-equilibrium emission is small, and the expansion of the source negligible. Furthermore, the emission of charged particles is limited temporally to the higher excitation energies, hence to the early stages by Coulomb barriers. With all these experimental conditions the spectra can provide a good measure of the temperature. Under any other conditions the separation of the unknown quantities becomes ambiguous and requires detailed models of the reaction mechanism.

3.4 Representative Measurements

In recent measurements of emitted fragments from intermediate energy heavy ion collisions, the slopes of the kinetic energy distributions of a large range of residues have been used to characterize the “temperatures” of moving sources. The remarkable finding is that this source generally has a slope parameter in MeV that is approximately equal to one-third of the bombarding energy per nucleon ($E/A_{projectile}$) independent

of the mass of the beam. The fact that the slope parameter tracks the bombarding energy is suggestive of injection of energy into internal degrees of freedom, and its dependence on $E/A_{\text{projectile}}$, rather than on $E/(A_{\text{projectile}}+A_{\text{target}})$ as expected for equilibration over the whole system, is attributed to the localization of the thermalization to the overlap zone of the projectile and target. In this model, the ratio of the number of “participants” to the number of particles in the whole system is given by geometry and does not depend strongly on the choice of initial system or bombarding energy. On the other hand, such a strong dependence on the velocity of the projectile (essentially E/A) may reflect an underlying contribution to the radial velocity of emitted ions from a direct scattering process.

The kinetic energy spectra of many particles types from our exemplary system $^{14}\text{N} + \text{Ag}$ at $E/A=35$ MeV have been reported(44, 25, 45, 46). These distributions fit very nicely into the moving source framework having fast projectile-like, intermediate velocity and slow target-like sources of particles. The slope parameters of the “intermediate source” are approximately 11-13 MeV. Therefore, before applying any other techniques to determine the apparent temperature of this source, there is nothing exceptional in the simple kinetic energy distributions of fragments from this reaction system. However, it should be recognized that problems have been indicated in the literature. Concentrating on the $^{14}\text{N} + \text{Ag}$ system, the emitted neutrons are not isotropic as required by the model(25) which points to the importance of angular momentum. Moreover, the neutron data are in good agreement with the predictions of a Boltzmann Master Equation model which does not introduce an intermediate source(36, 47, 48). Rather, the energetic particles are emitted continuously as the system moves towards equilibrium, after which the bulk of the particles are emitted.

4 Relative Yields of Different Species

4.1 Total Yields

We now consider manifestations of temperature in the relative yields of the various types of emitted species. The yields of two different fragments can be compared, of course, but such comparisons rely on detailed knowledge of the isospin dependence of the level densities. An equation similar to the Saha equation that is used to determine the ionization temperature in astrophysics (49) can be applied to the fragment yields. In such an equation the isotropic production cross section per degree of freedom is proportional to an exponential function of the separation energy, ϵ_s , divided by the temperature. Such analyses are sometimes referred to as “ Q_{gg} ” systematics because the separation energy is essentially the Q value for the emission of a given species from the emitting system. As before, a relatively simple expression for the distribution of isobars is obtained, but strong assumptions must be made about the nature of the emitting system in order to establish the actual value of ϵ_s for the emission of each fragment. Moreover, the experimental determinations of the ratio of yields have their own problems which are due to experimental biases associated with measuring fragments with different charges.

As a refinement, one might look at the yields of different stable isotopes of the same element. In principle this also would be determined by the difference in the separation energy of each isotope species according to the factor $\exp(-\epsilon_s/T)$. But there will also be a factor associated with the fact that different numbers of nucleons leave the source. This introduces changes in entropy which are associated with the change in particle number. In addition, the yields of light fragments are subject to ambiguities created by secondary (decay) events which follow the primary emission,

discussed below. The variation with Q value is dominated by the rapid changes in the binding energies of the light nuclei in actual measurements of the yields of light species. The exponential function, combined with averages over emitting system and experimental uncertainties, leads to a reasonable specification of the temperature. In specific measurements, the integrated yields are often well described by this Q_{gg} function. For example, the total yields of light products from the reaction of $^{58}\text{Ni} + ^{58}\text{Ni}$ (50) have been shown to be in good agreement with the predicted emission from a single compound nucleus, see Fig. 3.

In the case of $^{14}\text{N} + \text{Ag}$ at $E/A=35$ MeV, the temperature that was extracted from the distribution of integrated fragment yields of 8 ± 1 MeV was significantly below the kinetic energy temperature of 12 ± 2 MeV (44), see Table 1. An attempt to remove the sensitivity to the exact nature, mass and isospin, of the emitting source was made by taking ϵ_s to be the average Q value for fragment emission from a range of sources. Another recent calculation included a complete network of sequential decay feeding among the various emitted fragments, see below, which was fit to the integrated elemental and integrated isotopic yields(46). The expression $\epsilon_s = Q - fV_C$ was used in which Q was the difference in binding energies, V_C was the Coulomb potential between the light fragment and the residue, and f was adjusted at each temperature to reproduce the yields. The value of f varied systematically with temperature from a low of 0.85 at $T=2$ MeV to a high of 3.88 at $T=8$ MeV with similar representations of the data. Two points now become apparent, first, in neither case is the extracted temperature equal to the “slope parameter.” In both analyses the slope parameter has a significantly larger value. Second, these two analyses are not entirely inconsistent. Note that the higher temperature (8 MeV) obtained in the earlier work results from the lack of a Coulomb term in ϵ_s , and if the nominal value of $f = 1$ is used, then

the best value of T is $\approx 4\text{MeV}$. The relative yields are sensitive to the difference in V_C from channel to channel, so the results are in rough agreement because for these light fragments it happens that $\Delta V_C \approx Q$ (with large fluctuations). Because of these ambiguities, the total yield method has not been widely used by itself to determine temperatures. Rather, it plays a supporting role that is discussed below.

4.2 Yields of Bound Excited States

To a large extent the difficulties in determining the mass and isospin dependence of ϵ_s can be removed by considering the thermal population of states within a given residue that is emitted from the system. The effect of population of states within the large “daughter” is already contained in $\Gamma(E - \epsilon, A - n)$, however, this daughter usually is highly excited and continues to decay. Here we are considering specific states in the emitted species, now isolated by emission, that carry information about the temperature. We will focus on the ratio of two states, but the technique is general. Measuring the temperature by comparing the relative yields of the two states in one species also avoids many of the kinematic ambiguities inherent in spectral measurements.

In this restricted case we can safely assume that spin, isospin and dynamical aspects involved in the emission of each of the states is the same. These aspects include, the distribution of angular momentum, the distribution of source velocities, and Coulomb barriers. The principle remaining factor which distinguishes the yields of the states is again the separation energy, ϵ_s , associated with each state. Using Eq.8, the emission rate and total yield is determined by the factor $\exp(-\epsilon_s/T)$. The relative emission rate is simply $\exp(-\Delta\epsilon_s/T)$, where $\Delta\epsilon_s$ equals the difference in energy between the states. However, if the emission occurs from a source which

is cooling during the emission process, then the yields will be determined by the convolution of changing rates over the chain of emissions. If the emission rate is sharply peaked this may not pose a problem.

Pairs of levels usually do not have the same spin, particularly in light nuclei, and so the relative emission rate should include a factor for the ratio of the spin degeneracies. Thus, the ratio, R , of two levels in a single nucleus should be given by:

$$R = \frac{2J_u + 1}{2J_l + 1} \text{Exp}(-\Delta E/T) \quad (18)$$

where J_u and J_l are the spins of the upper and lower states, respectively, and $\Delta E = E_u - E_l$ is their energy separation. The variation of this ratio with temperature for the two bound states of ${}^7\text{Li}$ can be inferred from Fig. 4 that shows the fraction of nuclei in the excited state. At low temperatures the ratio rapidly increases and saturates at $R = \frac{2J_u+1}{2J_l+1} = \frac{1}{3}$ at high temperatures.

Consider for a moment measurements of the spectral shape and the yields of two states of a single specific fragment. The results from measurements using the ratios of yields will be dominated by the temperature associated with the greatest likelihood of emission. Whereas, the least ambiguous portion of the spectral measurement comes from the high energy tail which is determined by the highest temperatures in the reaction. These two temperatures, i.e., the highest and the one where emission is most likely, need not be the same. Furthermore, if there is emission before equilibrium is reached, this will also influence the spectra. However, the ratio of yields of two states may not be affected if the pre-equilibrium contribution to the yield is small.

The primary difficulty with the measurement of relative yields comes from subsequent redistribution of the population after the emission of the (small) fragment (51, 52, 53). The most important of these difficulties stems from the emission of

some other (intermediate mass) excited fragments which themselves decay into lighter fragments and substantially effect the (lighter) population ratios. The ratio of some populations may even become double valued due to increased feeding from increasing populations in highly excited unbound states in heavier emitted species. Thus, the determination of temperature from relative yields remains ambiguous unless the chain of secondary processes among emitted excited fragments is known. This requires a model of the emission process and detailed knowledge of the nuclear structure of the isotopes which take part. Finally it should be noted that even in the ideal case the sensitivity to the temperature is limited to values which are of the magnitude of the separation of energy of the two species that are measured. As indicated in Fig. 4, once the temperature exceeds this difference, ΔE , the relative yield becomes saturated, a phenomena that is well known in classical systems.

4.3 Measurements of Bound States

From a practical standpoint, it is very difficult to measure directly the ratio of bound states given in Eq.18 as the lifetimes of the γ -ray emitting states are generally short compared to the flight time of the particles. It is convenient to introduce the fraction, f , of a given type of nucleus that are observed to be in a bound excited state. This quantity is readily measured from the ratio of the number of observed γ -rays to the total number of the coincident fragments. The γ -ray fraction for a simple two-level system is then $f=R/(1+R)$. Similar γ -ray fractions can be measured for systems with a larger number of levels but more care is needed to account for cascading of transitions (54), see below. In a sense, such cascading of de-excitation transitions can be considered a close relative of feeding by particle emission from unbound states.

The first measurements of the emission of excited states of evaporated nuclei

were made of the bound states of ${}^6\text{Li}$, ${}^7\text{Li}$, and ${}^7\text{Be}$ nuclei(7). Such nuclei can be thought of as simple two-level systems that were in contact with the thermal bath before emission as each of these nuclei has effectively only one bound excited state. The population of the excited states was proposed as an independent test of the formation of an equilibrated hot zone previously assumed to be formed in intermediate energy reactions.(55, 23) These fragments were shown to have exponential kinetic energy distributions that followed the systematics, discussed above.

The first measurements of the gamma-ray fraction showed that relatively few nuclei were in the excited states(7, 44). In fact, the temperature obtained from the bound state populations ≈ 1 MeV was an order of magnitude lower than the slope parameters. As already indicated, the ratio of the relatively close spaced levels in these nuclei should have been saturated at such a high temperature. However, alternative production mechanisms, such as sequential decay worked out in detail by Hahn and Stöcker (56, 52, 53), or final state interactions after emission (51), could distort the distributions. Therefore, the application of the technique to highly excited systems did not adequately test the technique.

The validity of the technique was shown in several studies of the relative populations of fragments emitted from compound nuclei(57, 54, 58, 50, 59, 60). Using fragments from composite nuclear systems that have been thoroughly studied removes the uncertainty about the formation of the thermal nuclear system. For example, the production of the two-level systems of ${}^7\text{Li}$, ${}^7\text{Be}$ and ${}^6\text{Li}$ from the reaction of ${}^{12}\text{C} + {}^{14}\text{N}$ follows the predictions of thermal emission up to bombarding energies of $E/A \approx 10$ MeV (57) in good agreement with other measurements of this system (61). In a related study which used a slightly larger compound nucleus, Lee, *et al.* obtained similar results, as the relative populations of a broad range of nuclei were shown to be

in agreement with the predicted compound nucleus temperature when the bombarding energy was below approximately $E/A=10$ MeV(59, 60). At higher bombarding energies the relative populations of the excited states decreased, indicating preferential feeding of the ground states by another mechanism (sequential decay). In a related test, d'Onofrio,*et al.* measured the relative populations of ${}^7\text{Li}$ bound states from the reaction of ${}^{20}\text{Ne}$ with ${}^{60}\text{Ni}$ at $E/A = 36.2$ MeV (58). The population ratios of the fragments emitted at large angles were found to be nearly saturated and in agreement with the predictions of a Hauser-Feshbach formalism.

The γ -ray fraction for several states of a given emitted fragment was investigated by Sobotka *et al.* in the reaction of ${}^{19}\text{F} + {}^{159}\text{Tb}$ at 181 MeV. A measurement of the fractions as a function of particle kinetic energy was included. Importantly, the results generally indicated that the populations do not depend on kinetic energy, as expected or even required, for thermal equilibrium. However, a few fractions did depend on kinetic energy, but these were thought to be products of a binary peripheral process. These data also indicated substantial feeding of the ground states of the emitted fragments. Thus, internal ratios of the γ -ray fractions of two excited states, with appropriate cascade corrections, are more indicative of the compound nuclear temperature than fractions for single states (as the contribution from the ground state drops out in the ratio). Gomez del Campo, *et al.*, obtained an effective temperature of approximately 2 MeV from the relative fractions of single bound states in ${}^{12}\text{C}$, ${}^{15}\text{N}$, and ${}^{16}\text{O}$ from the reaction of ${}^{58}\text{Ni}$ with ${}^{58}\text{Ni}$ at $E/A=11$ MeV (50). These states are more widely separated than those in the lithium and beryllium nuclei. The effective temperature was, once again, less than the predicted compound nuclear temperature (4.1 MeV). However, detailed Hauser-Feshbach calculations (50, 62), shown to be in agreement with the integrated fragment yields for this reaction, mentioned above,

were able to calculate the sequential decay contribution to the population ratios and, therefore, the observed or effective temperature.

A comprehensive exploration of the various facets of thermal equilibrium evident in the distributions of bound-state populations was made by Xu, *et al.* for the reaction of $^{32}\text{S} + ^{nat}\text{Ag}$ with $E/A=22.3$ MeV (63, 64). The yields of fragments and the γ -ray fractions of a large number of widely separated or high-lying states was measured and compared to a comprehensive statistical model including all known decays with approximations for decay from the continua of products up to mass ~ 13 . Moreover, the predictions of the calculation were compared to the integrated elemental yields, the isotopic yields, and the γ -ray fractions so that the required overall agreement could be tested, somewhat similar to the analysis described in Ref. (50). The yields, γ -ray fractions, and even the ratios of the fractions of two states were shown to be in agreement with a temperature of $\approx 3\text{-}4$ MeV after substantial correction for sequential decay. The authors comment in their conclusions that agreement between the calculation and measurement may reflect more the accuracy of the sequential decay calculations than the accuracy of the thermal description (63). An example of the comparison of the γ -ray fractions to the model calculations is shown in Fig. 5.

Summarizing this section, the measurements of the ratios of bound states of emitted light fragments have been found to reflect the temperature of the emitting source provided that the temperature is relatively low, ≤ 1 MeV. Sequential decay of nearby light fragments preferentially increases the yield of the ground states thus simulating a lower temperature. This effect was observed both for closely and more widely spaced levels. Ratios of (bound) states that do not rely on the ground state were less sensitive to this problem. Comprehensive calculations including *all* sequential decay channels can account for the observed γ -ray fractions up to temperatures of ~ 4 MeV

but require extensive nuclear structure data as input.

4.4 *Yields of Unbound States*

With the development of experimental techniques to measure correlated pairs of particles, it is possible to make measurements of the relative yields of unbound as well as bound states of a given species. This extension provides two advantages over measurements with particle-stable states. First, the unbound states are generally more widely separated in energy than bound states which increases the saturation temperature and provides an opportunity to determine higher temperature values with greater precision. For example, comparison of states differing in energy of up to approximately 20 MeV are presented in Ref. (65). Second, it should be possible to reduce modification of the emitted populations by secondary decays by selecting the ratio for two unbound states. This reduces the major complication in determinations of the temperature with bound state populations.

Before measurement of the ratios of unbound (continuum) states one should explore a new contribution to the energy, namely the energy of the relative motion of the subfragments of the emitted system, which we will label as ϵ_r . For unbound states this is a continuous variable, and its treatment requires more care than that taken for the discrete energies of bound states (66, 46). Of particular concern is the factor $\Gamma(\epsilon, n)$ which appears in the expression for the probability, $P(\epsilon, n)$ in Eq.5. This factor represents the density of states for the emitted system and is primarily influenced by the interaction between these subfragments.

An analysis of the unbound density of states as a function of the relative energy, ϵ_r , can be performed with the same methods used in statistical mechanics for the determination of the second virial coefficient of interacting particles. The result is

that the density of states is modified from that of noninteracting particles to be

$$\Gamma(\epsilon, n) \propto \frac{1}{\pi}(2J + 1) \frac{\partial \delta_J}{\partial \epsilon_r}, \quad (19)$$

where δ_J is the phase shift in the channel labeled by the angular momentum J . If we assume a Breit-Wigner characterization of the resonant phase shifts, then we obtain

$$\Gamma(\epsilon, n) \propto \sum_i (2J_i + 1) \frac{1}{\pi} \frac{\Gamma_i/2}{(\epsilon_r - E_i)^2 + (\Gamma_i/2)^2}, \quad (20)$$

where the widths Γ_i , energies E_i , and angular momenta J_i are associated with the resonant states. The integration over the relative energy for each resonant state provides a value of 1.0. Thus, for counting purposes, each resonant state has unit weight. The second factor in $P(\epsilon, n)$, i.e. $\Gamma(E - \epsilon, A - n)$ provides the proportionality to $\exp(-\epsilon_r/T)$, which has the same origin as the factors $\exp(-\epsilon_k/T)$ for spectra and $\exp(-\epsilon_s/T)$ for bound states, discussed above. Under the assumption that the emitted species is in equilibrium with the large residual daughter as before, one would expect the yield as function of relative energy for two-particle continuum states of the emitted species, ϵ_r , to be given by:

$$\sum_i (2J_i + 1) \frac{1}{\pi} \frac{\Gamma_i/2}{(\epsilon_r - E_i)^2 + (\Gamma_i/2)^2} \exp(-\epsilon_r/T). \quad (21)$$

This form has been compared to the measured yields to extract the temperature. This form has also been used to compare the yields of states in different two-particle channels.

4.5 Measurements of Unbound States

Relatively soon after the first measurements of the bound excited state populations were reported, measurements of the unbound states of light fragments were obtained(65, 67). These measurements are technically more difficult as they are based

on the measurement of the relative momenta of coincident light particles. A large number of studies of a range of reaction systems have been carried out with pairs of charged particles (65, 67, 68, 69, 70, 71, 66, 72, 73, 74, 75, 76, 77, 46, 78, 79, 80, 81) and also with neutron-charged particle pairs (82, 83, 84, 85). These studies have concentrated on intermediate energy reactions that produce relatively high excitation energies and thus emit large numbers of intermediate mass fragments in unbound states. Unfortunately, a direct calibration of the technique by studying a well known compound-nuclear system has not been done. However, Natowitz, *et al.* have recently collected the measurements of emitted unbound populations from highly excited nuclei with $A \simeq 120$ and produced an “intercalibration” (86).

The detection of unbound states itself implies that sequential decay is an important process in the production of these self-same nuclei. Therefore, the analyses of these data have incorporated sophisticated Hauser-Feshbach calculations of the total isotopic yields and internal feeding. In general, the temperatures extracted from these analyses have provided predictions of the isotopic yields and the unbound levels in one framework.

The measurements of coincident pairs of particles have additional technical difficulties that arise when evaluating the coincidence efficiency function. The treatment of pairs of charged particle and neutron-charged particle pairs is slightly different, and we will discuss each separately. First, let us consider the measurements of unbound excited states that decay into pairs of charged particles. These particles are detected in large hodoscope arrays of individual charged particle telescopes that were originally developed for correlation function measurements. The data are binned according to the relative momentum, q , of the two particles, and the distribution contains an underlying background and peaks which correspond to the unbound resonances. The

coincidence decay yield of an unstable state, labeled Y_c , is extracted from the the total yield of a given pair by subtraction of the underlying background correction function(65). The decay yield is linked to the initial populations through the detection efficiency, $\epsilon(E^*, E)$, where E^* is the excitation energy and E is the observed relative energy. The efficiency has been estimated in Monte Carlo calculations which include the precise geometry, detection thresholds and energy resolution, cf. (65, 46). The yield as a function of temperature is then:

$$Y_c(E_{mea}^*) = \int dE^* \epsilon(E^*, E_{mea}^*) \frac{dn(E^*)}{dE^*} \quad 22$$

where E^* the actual excitation energy and $dn(E^*)/dE^*$ is the excitation energy spectrum and is therefore a sum over the resonances that contribute to the spectrum including their widths and branching ratios. A detailed discussion of $dn(E^*)/dE^*$ has been given by Nayak, *et al.* (46). As an example, Fig. 6 shows the $\alpha+{}^6\text{Li}$ and the $p+{}^9\text{Be}$ excitation energy spectra from the decay of excited ${}^{10}\text{B}$ fragments. Notice the offset in the proton channel due to the higher separation energy. Such data is extremely powerful in evaluating the effects of the efficiency function because several decay channels can be detected from some emitted fragments.

The range of unstable states and the reaction systems that have been measured is quite large. Even in a single reaction system the detectors will accept a large variety of charged particles that can be analyzed in this framework. Thus, a “second level” chi-squared analysis in which the best temperature is determined for all the observed states has been performed in the more recent measurements (46, 78), similar to analyses of reactions in which a large numbers of bound states were measured (63). For example, the distribution of the excited states in ${}^{10}\text{B}$ nuclei produced in the reaction of ${}^{36}\text{Ar} + {}^{197}\text{Au}$ is shown in Fig. 7 from Ref. (78). Overall, the data are well described by a temperature of 4 MeV, but notice that the measured yield of the state

near 6 MeV is too large. The yields have been divided by the spin degeneracy, so the excess production could represent a population inversion, an incorrect spin assignment in the literature, or population of an unknown state. The predicted modification of the distribution by sequential decay is also indicated in the figure by the difference of the open boxes from the dashed line.

From a broad perspective, all of the measurements of the populations of unbound states have the interesting feature that the temperature appears to reach an upper limit of approximately 6 MeV. These measurements have included a broad range of reactions, some with very large nuclei, and with large bombarding energies, and most of these had slope parameters much in excess of 6 MeV. This limit could be an indication of the onset of multifragmentation, in effect, a phase transition.

Measurements of neutron unbound states have been made by detecting charged particles and neutrons in a colinear geometry and analyzing the relative velocity spectrum (82). Such a spectrum also contains two components: neutrons emitted from discrete states, and a continuous background of neutrons emitted from other sources (such as the heavy residue). The background has been determined with less ambiguity than that in the charged particle data by fitting the neutron spectra observed in coincidence with a given fragment at all angles, see for example Ref. (82, 83), and then transforming the analytical form into the relative velocity spectrum. An example of such a transformation is shown in Fig. 8. The colinear geometry with a narrow acceptance causes each decay to split into two peaks, faster neutrons having been emitted near 0° in the moving frame and slower neutrons emitted near 180° .

A more complicated relative velocity spectrum from Ref. (85) is shown in Fig. 9 for the decay of $^{13}\text{C}^*$ into $^{12}\text{C} + n$. The positions of the peaks are determined by the decay energy, and the relative areas are determined by the detection efficiency

and the state populations. The technique is most sensitive to low energy transitions that produce neutrons and charged particles with small relative velocities. Therefore, decays from higher lying excited states to the first excited state in the daughter have been seen, as shown for $^{13}\text{C}^*$.

The studies of neutron unbound states have concentrated on the reaction of $^{14}\text{N} + \text{Ag}$ at $E/A=35$ MeV. They have shown that the source of the fragments emitted at large angles with exponential spectra has a temperature of approximately 3 MeV (85, 83). Clear evidence has also been shown for a kinetic energy dependence of the level populations at forward angles, attributed to the importance of projectile excitation and decay (85).

Bloch, *et al.*, have been able to combine the results of their lithium-neutron coincidence measurements (83) with the results of the earlier measurements of the bound state populations of ^7Li in a uniform picture. The populations of the bound states, an unbound state, and the feeding from neutron decay of ^8Li were found to be consistent with a single temperature of approximately 3 MeV when the *total* feeding to the ground state was included. Thus, the bulk of the data for the $^{14}\text{N} + \text{Ag}$ at $E/A=35$ MeV reaction indicates the production of a large nuclear system at thermal equilibrium with a temperature on the order of 3 MeV. Dabrowski, *et al.* found a similar agreement between the population temperatures and the slope parameter of the slow source (target-like fragment) for the reaction of $^{40}\text{Ar} + \text{Ag}$ with $E/A = 44$ MeV. Thus, the harder spectral slopes must be due to pre-equilibrium decay and the dynamical enhancement of the kinetic energy from angular momentum, etc., and not thermal equilibrium.

Very recently, the excited state production method has been extended to relative production of the $\Delta(1232)$ resonance and nucleons in ultra-relativistic heavy-ion

collisions (87, 88). Using the assumption of a thermal source for these baryons, the population of nucleon resonances becomes a function of temperature. The relative population of the Delta(1232) resonance was extracted from the measured pion distributions and is consistent with a temperature of 140 MeV !

5 Conclusions

The measurement of nuclear temperatures in heavy-ion reactions has a long and rich history. The simplest measurements of the slope-parameters of kinetic energy distributions is well founded in thermal evaporation theory with the ansatz of “sudden disintegration of an equilibrated source.” The model can be fit to a broad range of data and is supported by a systematic variation of the parameters with bombarding energy. Following on the apparent success of this thermal description, many studies have been made of other features which are consistent with thermal equilibrium, most significantly the populations of excited states of emitted nuclei. These internal populations are least sensitive to potentially unknown or uncontrollable aspects of the fragment production mechanism.

The apparent thermal population of the unbound excited states of emitted light nuclei has been clearly demonstrated in recent years. The populations of the states have been shown to follow the simple Boltzmann distributions but are substantially modified by sequential decay at high temperature. Population ratios containing the ground state have been shown to be particularly sensitive to perturbation by feeding from unbound levels. The distributions of bound states have been shown to follow the compound nuclear temperature up to about 2 MeV but are not useful at higher temperatures due to the typically small level spacing and the difficulties created by feeding. The populations of unbound levels are generally more widely separated and

are less subject to feeding (in fact, they represent the feeding). A large number of population ratios have been measured with both neutron and charged particle decay channels. Overall, the results show that the temperatures of the emitting nuclei do not exceed approximately 6 MeV even when the slope parameters are many times larger. This discrepancy is most likely due to contributions to the kinetic energy of the particles from collective motion that is not thermalized during the collision but is not quantitatively understood at present.

During the last ten years the concept of nuclear temperature and the methods of studying it have received considerable attention in the field of heavy ion reactions. The reason for this interest is that equilibrium and temperature represent central concepts in the thermodynamic description of the reactions and their evolution. Although not all the problems associated with the subject have been solved, we have shown that studies of temperature and equilibrium have lead to considerable progress in understanding reaction mechanisms. The field has come a long way since the era in which the temperature of the system was assumed to be the slope parameter of the particle spectrum. The addition of other methods of measurement within the thermodynamic framework has revealed a rich collection of new phenomena, which are now being treated in the models of the reactions. The eventual goal of the field, to specify the thermodynamic properties of nuclear matter itself, has been and will continue to be significantly advanced by these inquiries.

6 Acknowledgements

The authors would like to express their thanks to numerous collaborators for many discussions on the subject of this review. This work was partially supported by the cooperative agreement numbers PHY-9017077 and PHY-9015255 from the National

Science Foundation.

Literature cited

1. H.A. Bethe, *Rev. Mod. Phys.* **9** 69-244 (1937).
2. V.F. Weisskopf, *Phys. Rev.* **52**: 295-303 (1937.)
3. E. Suraud, Ch. Grégoire, and B. Tamain, *Prog. Part. and Nucl. Phys.* **23**, 357-467 (1989).
4. B. Tamian, *Proc. Intl. Sch. of Phys. CXII, Varenna*, (North Holland, 1991) 1-36.
5. R.G. Stokstad, in *Treatise on Heavy-Ion Science*, D.A. Bromley, Ed. (Plenum Press, New York, 1984), Vol. 3, Ch. 2. 83-197.
6. W. Hauser and H. Feshbach, *Phys. Rev.* **87**: 366-373 (1952.)
7. D.J. Morrissey, W. Benenson, E. Kashy, B. Sherrill, A.D. Panagiotou, R.A. Blue, R.M. Ronningen, J. van der Plicht, and H. Utsunomiya, *Phys. Lett.* **B148**: 423-427 (1984.)
8. K. Huang, *Statistical Mechanics*, 2ndEd. (John Wiley & Sons, New York, 1987).
9. A. Gilbert, and A.G.W. Cameron, *Can. J. Phys.* **43**: 1446-1496 (1965.)
10. J.R. Huizenga, and L.G. Moretto, *Ann. Rev. Nucl. Sci.* **22**: 427-464 (1972.)
11. W.A. Friedman and W.G. Lynch, *Phys. Rev.* **C28**: 16-23 (1983.)
12. W.A. Friedman, *Phys. Rev. Lett.* **60**: 2125-2128 (1988.)
13. S. Shlomo, *Nucl. Phys.* **A539**: 17-36 (1992.)

14. S. Shlomo, and J.B. Natowitz, *Phys. Rev. C*44: 2878-2880 (1991.)
15. S. Shlomo, and J.B. Natowitz, *Phys. Lett. B*252: 187-191 (1990.)
16. D.L. Tubbs and S.E. Koonin, *Ap.J.* **232** L59 (1979).
17. P. Bonch, S. Levit, and D. Vautherin, *Nucl. Phys. A*427: 278-296 (1984.)
18. M.G. Mustafa, M. Blann, A.V. Ignatyuk, and S.M. Grimes, *Phys. Rev. C*45: 1078-1083 ((1992).)
19. L. Rosen and L. Stewart, *Phys. Rev.* 99: 1052-1053 (1955.)
20. F.L. Ribe, in *Fast Neutron Physics, Part II*, J.B. Marion, and J.L. Fowler, Eds. (John Wiley & Sons, New York, 1963), Ch. V.N 1775-1864.
21. G.D. Westfall, J. Gosset, P.J. Johansen, A.M. Poskanzer, W.G. Meyer, H.H. Gutbrod, A. Sandoval, and R. Stock, *Phys. Rev. Lett.* 37: 1202-1205 (1976.)
22. G.D. Westfall, B.V. Jacak, N. Anantaraman, M.W. Curtin, G.M. Crawley, C.K. Gelbke, B. Hasselquist, W.G. Lynch, D.K. Scott, B.M. Tsang, M.J. Murphy, T.J.M. Symons, R. Legrain, and T.J. Majors, *Phys. Lett. B*116: 118-122 (1982.)
23. B.V. Jacak, G.D. Westfall, C.K. Gelbke, L.H. Harwood, W.G. Lynch, D.K. Scott, H. Stöker, M.B. Tsang, and T.J.M. Symons, *Phys. Rev. Lett.* 51: 1846-1849 (1983.)
24. D.J. Fields, W.G. Lynch, C.B. Chitwood, C.K. Gelbke, M.B. Tsang, H. Utsunomiya, and J. Aichelin, *Phys. Rev. C*30: 1912-1923 (1984.)
25. C. Bloch, W. Benenson, A.I. Galonsky, E. Kashy, J. Heltsley, L. Heilbronn, M. Lowe, R.J. Radtke, B. Remington, J. Kasagi, D.J. Morrissey, *Phys. Rev. C*37: 2469-2486 (1988.)

26. R. Wada, D. Fabris, K. Hagel, G. Nebbia, Y. Lou, M. Gonin, J.B. Natowitz, R. Billery, B. Cheynis, A. Demeyer, D. Drain, G. Guinet, C. Pastor, L. Vagneron, K. Zaid, J. Alarja, A. Giorni, D. Heuer, C. Morand, B. Viano, C. Mazur, C. Ngo, S. Leray, R. Lucas, M. Ribrag and E. Tomasi *Phys. Rev. C*39: 497-515 (1989.)
27. M. Gonin, L. Cooke, K. Hagel, J.B. Natowitz, R.P. Schmitt, S. Schlomo, B. Srivastava, W. Turmel, H. Utsunomiya, R. Wada, G. Nardelli, G. Nebbia, G. Viesti, R. Zanon, B. Fornal, G. Prete, K. Niita, S. Hannuschke, P. Gonthier, and B. Wilkins, *Phys. Rev. C*42: 2125-2142 (1990.)
28. D. Cussol, G. Bizard, R. Brou, D. Durand, M. Louvel, J.P. Patry, J. Péter, J.P. Sullivan, R. Regimbart, J.C. Steckmeyer, B. Tamain, E. Crema, H. Doubre, G.M. Jin, K. Hagel, A. Péghaire, F. Saint-Laurent, Y. Cassagnou, R. Legrain, C. Lebrun, E. Rosato, R. MacGrath, S.C. Jeong, S.M. Lee, Y. Nagashima, T. Nakagawa, M. Ohihara, J. Kasagi, and T. Motobayashi, *Nucl. Phys. A* submitted: for publication (1992.)
29. M. Louvel, T. Hamdani, G. Bizard, R. Bougault, R. Brou, H. Doubre, D. Durand, Y. El Masri, H. Fugiwara, A. Genoux-Lubain, K. Hagel, A. Hajfani, F. Hanappe, S.C. Jeong, G.M. Jin, S. Kato, J.L. Laville, C. Le Brun, J.F. Lecolley, S. Lee, T. Matsuse, T. Motobayashi, J.P. Patry, A. Péghaire, J. Péter, N. Prot, R. Regimbard, F. Saint-Laurent, J.C. Steckmeyer, and B. Tamian, *Nucl. Phys. A* submitted: for publication (1992.)
30. M. Gonin, L. Cooke, K. Hagel, Y. Lou, J.B. Natowitz, R.P. Schmitt, B. Srivastava, W. Turmel, H. Utsunomiya, R. Wada, B. Fornal, G. Nardelli, G. Nebbia, G. Viesti, R. Zanon, G. Prete, P. Gonthier, and B. Wilkins, *Phys. Lett. B*217: 406-410 (1989.)

31. E. Crema, S. Bresson, H. Doubre, J. Galin, B. Gatty, D. Guerreau, D. Jacquet, U. Jahnke, B. Lott, M. Morjean, E. Piasecki, J. Pouthas, F. Saint-Laurent, E. Schwin, A. Sokolov, and X.M. Wang, *Phys. Lett. B*258: 266-270 (1991.)
32. J.B. Natowitz, *Nucl. Phys. A*482: 171c-186c (1988.)
33. I. Dostrovsky, P. Rabinowitz, and R. Bivins, *Phys. Rev.* 111: 1659-1676 (1958.)
34. R. Pühlhofer, *Nucl. Phys. A*280: 267-284 (1977.)
35. A. Gavron, *Phys. Rev. C*21: 230-236 (1980.)
36. M. Blann, *Phys. Rev. C*23: 205-212 (1981.)
37. R.J. Charity, M.A. McMahan, G.J. Wozniak, R.J. McDonald, L.G. Moretto, D.G. Sarantites, L.G. Sobotka, G. Guarino, A. Pantaleo, L. Fiore, A. Gobbi, and K.D. Hildebrand, *Nucl. Phys. A*483: 371-405 (1988.)
38. J.R. Grover, and J. Gilat, *Phys. Rev.* 157: 802-813 (1962.)
39. M. Blann, *Phys. Rev.* 157: 860-870 (1967.)
40. W.A. Friedman, *Phys. Rev. C*37: 976-984 (1988.)
41. C.B. Chitwood, D.J. Fields, C.K. Gelbke, D.R. Klesh, W.G. Lynch, M.B. Tsang, T.C. Awes, R.L. Ferguson, F.E. Obenshain, F. Plasil, R.L. Robinson, and G.R. Young, *Phys. Rev. C*34: 858-871 (1986.)
42. P.J. Siemens, and J.O. Rasmussen, *Phys. Rev. Lett.* 42: 880-883 (1979.)
43. W.A. Friedman, *Phys. Rev. C*42: 667-673 (1990.)
44. D.J. Morrissey, W. Benenson, E. Kashy, C. Bloch, M. Lowe, R.A. Blue, R.M. Ronningen, B. Sherrill, H. Utsunomiya, I. Kelson, *Phys. Rev. C*32: 877-886 (1985.)

45. F. Deák, Á. Kiss, Z. Seres, A. Galonsky, L. Heilbronn, and H. Schelin, *Phys. Rev. C*42: 1029-1035 (1990.)
46. T.K. Nayak, T. Murakami, W.G. Lynch, K. Swartz, D.J. Fields, C.K. Gelbke, Y.D. Kim, J. Pochodzalla, M.B. Tsang, H.M. Xu, F. Zhu, K. Kwiatkowski, *Phys. Rev. C*45: 132-161 (1992.)
47. H. Machner, *Z. Phys. A*321: 577-580 (1985.)
48. H. Machner, *Phys. Rev. C*127: 309-377 (1985.)
49. D.D. Clayton, *Principles of Stellar Evolution and Nucleosynthesis* (McGraw-Hill, New York, 1968).
50. J. Gomez del Campo, J.L. Charvet, A. D'Onofrio, R.L. Auble, J.R. Beene, M.L. Halbert, J.H. Kim, *Phys. Rev. Lett.* 61: 290-293 (1988.)
51. D.H. Boal, *Phys. Rev. C*30: 749-751 (1984.)
52. D. Hahn, and H. Stöcker, *Phys. Rev. C*35: 1311-1315 (1987.)
53. D. Hahn, and H. Stöcker, *Nucl. Phys. A*476: 718-772 (1988.)
54. L.G. Sobotka, D.G. Sarantites, H. Puchta, F.A. Dilmanian, M. Jääkeläinen, M.L. Halbert, J.H. Barker, J.R. Beene, R.L. Ferguson, D.C. Hensley, and G.R. Young, *Phys. Rev. C*34: 917-924 (1986.)
55. C.B. Chitwood, D.J. Fields, C.K. Gelbke, W.G. Lynch, A.D. Panagiotou, M.B. Tsang, H. Utsunomiya, and W.A. Friedman, *Phys. Lett. B*131: 289-291 (1983.)
56. H. Stöcker, G. Buchwald, G. Graebner, P. Subramanian, J.A. Maruhn, W. Greiner, B.V. Jacak, and G.D. Westfall, *Nucl. Phys. A*400: 63c-93c (1983.)

57. D.J. Morrissey, C. Bloch, W. Benenson, E. Kashy, R.A. Blue, R.M. Ronningen, R. Aryaeinejad, *Phys. Rev. C*34: 761-763 (1986.)
58. A. d'Onofrio, B. Delaunay, J. Delaunay, H. Dumont, J. Gomez del Campo, A. Brondi, R. Moro, M. Romano, F. Terrasi, J.F. Bruandet, *Z. Phys. A*326: 335-336 (1987.)
59. J.H. Lee, W. Benenson, D.J. Morrissey, *Phys. Rev. C*41: 1562-1575 (1990.)
60. J.H. Lee, W. Benenson, C. Bloch, Y. Chen, R.J. Radtke, E. Kashy, M.F. Mohar, D.J. Morrissey, R. Blue, R.M. Ronningen, *Phys. Rev. C*41: 2406-2409 (1990.)
61. J. Gomez del Campo, R.G. Stokstad, J.A. Biggerstaff, R.A. Dayras, A.H. Snell, and P.H. Stelson, *Phys. Rev. C*19: 2170-2185 (1979), and references therein.
62. J. Gomez del Campo, *Bul. Am. Phys. Soc.* 31 770 (1986), and private communication.
63. H.M. Xu, W.G. Lynch, C.K. Gelbke, M.B. Tsang, D.J. Fields, M.R. Maier, D.J. Morrissey, T.K. Nayak, J. Pochodzalla, D.G. Sarantites, L.G. Sobotka, M.L. Halbert, D.C. Hensley, *Phys. Rev. C*40: 186-210 (1989.)
64. H.M. Xu, D.J. Fields, W.G. Lynch, M. B. Tsang, C.K. Gelbke, M.R. Maier, D.J. Morrissey, J. Pochodzalla, D.G. Sarantites, L.G. Sobotka, M.L. Halbert, D.C. Hensley, D. Hahn, H. Stocker, *Phys. Lett.* B182: 155-158 (1986.)
65. J. Pochodzalla, W.A. Friedman, C.K. Gelbke, W.G. Lynch, M. Maier, D. Ardouin, H. Delagrangé, H. Doubre, C. Gregoire, A. Kyanowski, W. Mitting, A. Peghaire, J. Peter, F. Saint-Laurent, Y.P. Viyogi, B. Zwieglinski, G. Bizard, F. Lefebvres, B. Tamain, J. Quebert, *Phys. Rev.* B161: 275-279 (1985.)

66. J. Pochodzalla, C.K. Gelbke, W.G. Lynch, M. Maier, D. Ardouin, H. Delagrange, H. Doubre, C. Grégoire, A. Kyanowski, W. Mittig, A. Péghaire, J. Péter, F. Saint-Laurent, B. Zwięglinski, G. Bizard, F. Lefèbvres, B. Tamain, J. Québert, Y.P. Viyogi, W.A. Friedman, D.H. Boal, *Phys. Rev. C*35: 1695-1719 (1987.)
67. J. Pochodzalla, W.A. Friedman, C.K. Gelbke, W.G. Lynch, M. Maier, D. Ardouin, H. Delagrange, H. Doubre, C. Gregoire, A. Kyanowski, W. Mittig, A. Peghaire, J. Peter, F. Saint-Laurent, Y.P. Viyogi, B. Zwięglinski, G. Bizard, F. Lefebvres, B. Tamain, J. Quebert, *Phys. Rev. Lett.* 55: 177-180 (1985.)
68. C.B. Chitwood, C.K. Gelbke, J. Pochodzalla, Z. Chen, D.J. Fields, W.G. Lynch, R. Morse, M.B. Tsang, D.H. Boal, J.C. Shillcock, *Phys. Lett.* B172: 27-31 (1986.)
69. Z. Chen, C.K. Gelbke, J. Pochodzalla, C.B. Chitwood, D.J. Fields, W.G. Gong, W.G. Lynch, M.B. Tsang, *Nucl. Phys.* A473: 564-594 (1987.)
70. Z. Chen, C.K. Gelbke, W.G. Gong, Y.D. Kim, W.G. Lynch, M.R. Maier, J. Pochodzalla, M.B. Tsang, F. Saint-Laurent, D. Ardouin, H. Delagrange, H. Doubre, J. Kasagi, A. Kyanowski, A. Péghaire, J. Péter, E. Rosato, G. Bizard, F. Lefèbvres, B. Tamain, J. Québert, Y.P. Viyogi, *Phys. Lett.* B199: 171-175 (1987.)
71. Z. Chen, C.K. Gelbke, W.G. Gong, Y.D. Kim, W.G. Lynch, M.R. Maier, J. Pochodzalla, M.B. Tsang, F. Saint-Laurent, D. Ardouin, H. Delagrange, H. Doubre, J. Kasagi, A. Kyanowski, A. Péghaire, J. Péter, E. Rosato, G. Bizard, F. Lefèbvres, B. Tamain, J. Québert, Y.P. Viyogi, *Phys. Rev. C*36: 2297-2308 (1987.)
72. F. Saint-Laurent, A. Kyanowski, D. Ardouin, H. Delagrange, H. Doubre, C. Grégoire, W. Mittig, A. Péghaire, J. Péter, G. Bizard, F. Lefèbvres, B. Tamain,

- J. Québert, Y.P. Viyogi, J. Pochodzalla, C.K. Gelbke, W. Lynch, M. Maier, *Phys. Lett. B*202: 190-193 (1988.)
73. D.A. Cebra, W. Benenson, Y. Chen, E. Kashy, A. Pradhan, A. Vander Molen, G.D. Westfall, W.K. Wilson, D.J. Morrissey, R.S. Tickle, R. Korteling, R.L. Helmer, *Phys. Lett. B*227: 336-340 (1989.)
74. T. Murakami, T.K. Nayak, W.G. Lynch, K. Swartz, D.J. Fields, C.K. Gelbke, Y.D. Kim, K. Kwiatkowski, J. Pochodzalla, M.B. Tsang, F. Zhu, *J. Phys. Soc. Jpn.* 58: Suppl. 693-698 (1989.)
75. T.K. Nayak, T. Murakami, W.G. Lynch, K. Swartz, D.J. Fields, C.K. Gelbke, Y.D. Kim, J. Pochodzalla, M.B. Tsang, H.M. Xu, F. Zhu, K. Kwiatkowski, *Phys. Rev. Lett.* 62: 1021-1024 (1989.)
76. H. Dabrowski, D. Goujdami, F. Guilbalt, C. Lebrun, D. Ardouin, P. Lautridou, R. Boisgard, J. Québert, A. Péghaire, P. Eudes, F. Sébille, and B. Remaud, *Phys. Lett. B*247: 223-227 (1990.)
77. G.J. Kunde, J. Pochodzalla, J. Aichelin, E. Berdermann, B. Berthier, C. Cerruti, C.K. Gelbke, J. Hubele, P. Kreutz, S. Leray, R. Lucas, U. Lynen, U. Milkau, W.F.J. Müller, C. Ngô, C.H. Pinkenburg, G. Raciti, H. Sann, and W. Trautmann, *Phys. Lett. B*272: 202-206 (1991.)
78. F. Zhu, W.G. Lynch, D.R. Bowman, R.T. de Souza, C.K. Gelbke, Y.D. Kim, L. Phair, M.B. Tsang, C. Williams, H.M. Xu, J. Dinius, *Phys. Lett. B*282: 299-304 (1992.)
79. C. Schwarz, W.G. Gong, N. Carlin, C.K. Gelbke, Y.D. Kim, W.G. Lynch, T. Murakami, G. Poggi, R.T. de Souza, M.B. Tsang, H.M. Xu, D.E. Fields, K.

- Kwiatkowski, V.E. Viola, Jr., and S.J. Yennello, *Phys. Rev. C*48: 676-687 (1993.)
80. H. Xi, W. Zhan, Y. Zhu, Z. Guo, X. Hu, G. Liu, J. Zhou, S. Yin, Y. Zhao, Z. Wei, and E. Fan, *Nucl. Phys. A*552: 281-292 (1993.)
81. F. Zhu, M.J. Huang, W.G. Lynch, T. Murakami, Y.D. Kim, T.K. Nayak, R. Pelak, M.B. Tsang, H.M. Xu, W.G. Gong, K. Kwiatkowski, R. Planeta, S. Rose, V.E. Viola, Jr., L.W. Woo, S. J. Yennello, and J. Zhang, *Phys. Lett. B* submitted: for publication (1993.)
82. A. Galonsky, G. Casky, L. Heilbronn, B. Remington, H. Schelin, F. Deák, Á. Kiss, Z. Seres, and J. Kasagi, *Phys. Lett. B*197: 511-514 (1987.)
83. C. Bloch, W. Benenson, A.I. Galonsky, E. Kashy, J. Heltsley, L. Heilbronn, M. Lowe, B. Remington, D.J. Morrissey, J. Kasagi, *Phys. Rev. C*36: 203-207 (1987.)
84. F. Deák, A. Kiss, Z. Seres, A. Galonsky, C.K. Gelbke, L. Heilbronn, W.G. Lynch, T. Murakami, H. Schelin, M.B. Tsang, B.A. Remington, J. Kasagi, *Phys. Rev. C*39: 733-736 (1989.)
85. L. Heilbronn, A. Galonsky, C.K. Gelbke, W.G. Lynch, T. Murakami, D. Sackett, H. Schelin, M.B. Tsang, F. Deak, A. Kiss, Z. Seres, J. Kasagi, B.A. Remington, *Phys. Rev. C*43: 2318-2334 (1991.)
86. J.B. Natowitz, J.C. Hagel, R. Wada, X. Bin, J. Li, Y. Lou, and D. Utley, *Phys. Rev. C*43: 2074-2077 (1993.)
87. P. Braun-Munzinger, and the E814/E877 Collaboration, Proc. NATO Adv. Inst. on "Hot and Dense Nuclear Matter," Bodrum, Turkey, Oct., 1993, (Plenum, New York), in press.

88. J. Stachel, for the E814 Collaboration, Proc. Quark Matter-93, *Nucl. Phys.* in press (1994).

Table 1: Overview of the nuclear temperature measurements for the reaction of ^{14}N with ^{nat}Ag at $E/A=35$ MeV.

Observed Quantity	Angular Range	Temperature	Reference
Charged Particle Spectra	90-110°	8.6 MeV	(7)
	50-90°	12±2	(44)
	50-90°	13±2	(25)
	15-83°	13±1	(45)
	31-46°	~ 12†	(46)
Coincident Neutron Spectra	20-160°	3,12 MeV	(25)
	15-83°	10±2	(45)
Fragment Isotopic Yields	90-110°	8±1 MeV‡	(44)
	31-46°	4 ‡	(46)
Bound State Populations	50-90°	~1 MeV	(44)
	50-90°	~1 MeV	(83)
Neutron Unbound States	50°	3 MeV	(83)
Charged Particle Unbound States	31-46°	3-4 MeV	(46)

† Somewhat ambiguous due to limited angular range.

‡ The difference between these two analyses is the treatment of the Coulomb energy, see the text.

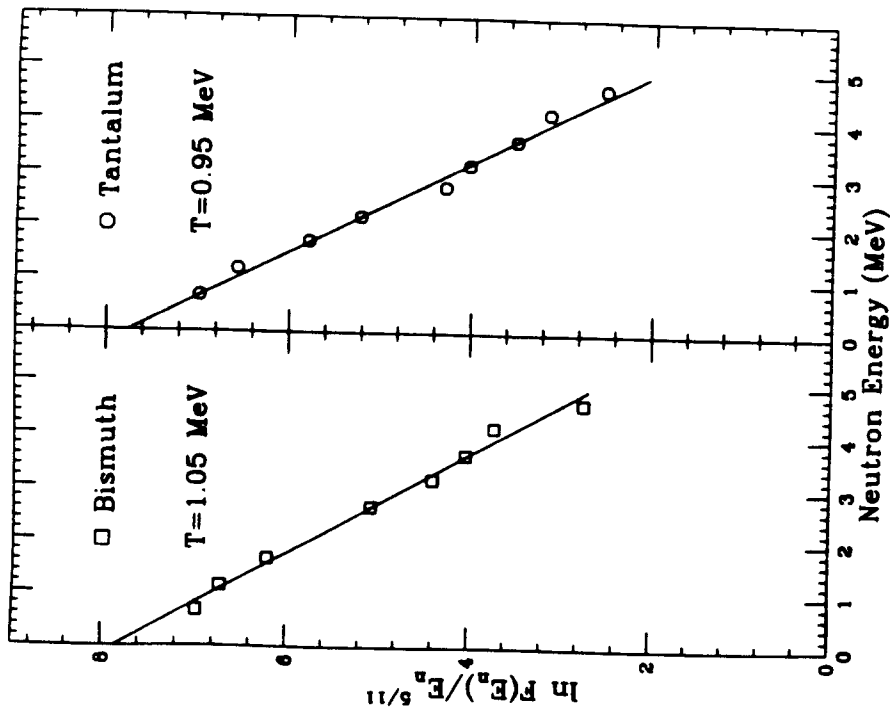


Figure 1 The spectrum of neutrons produced in the reaction of 14 MeV neutrons with bismuth and tantalum obtained by Rosen and Stewart (19), after a figure from Ribe (20). The reaction is dominated by single neutron emission with a small component of two neutron emission. The ordinate has been divided by the appropriate preexponential factor to emphasize the exponential slope.

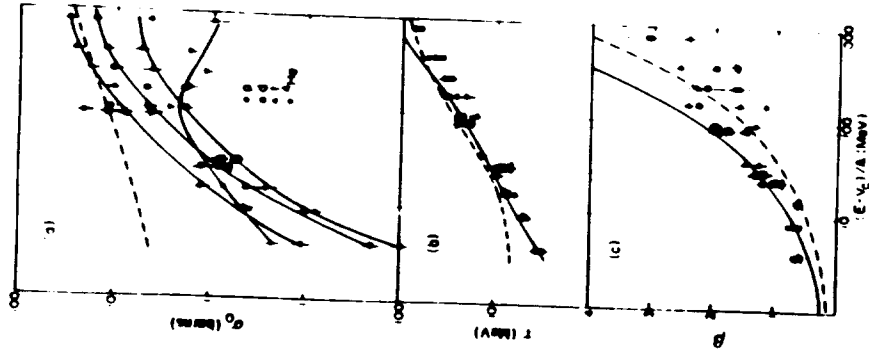


Figure 2 A summary of the analysis of inclusive charged particle spectra in the moving source framework(22). The variation of the three fitted parameters, the total cross section, σ , the slope parameter, r , and the parallel velocity, β , is shown as a function of the bombarding energy. The curves are predictions from a thermal model with "sudden disintegration" as described in Ref (22).

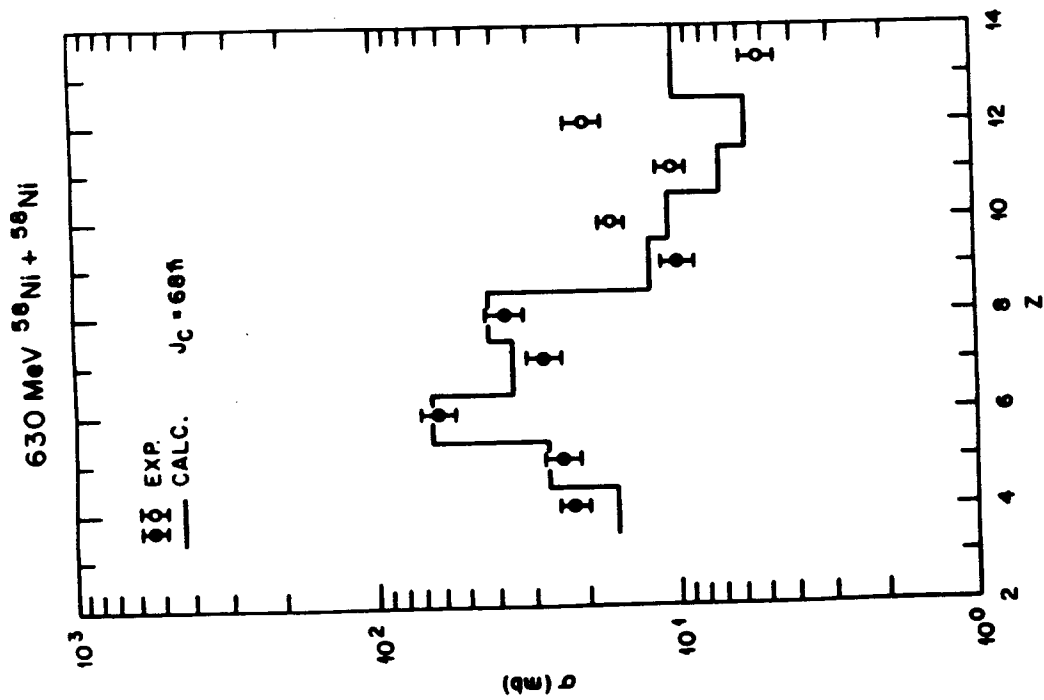


Figure 3 The angle integrated yield of light nuclei from the reaction of $^{56}\text{Ni} + ^{56}\text{Ni}$ at $E=630$ MeV from (90). The measured yields compare well to the predictions of

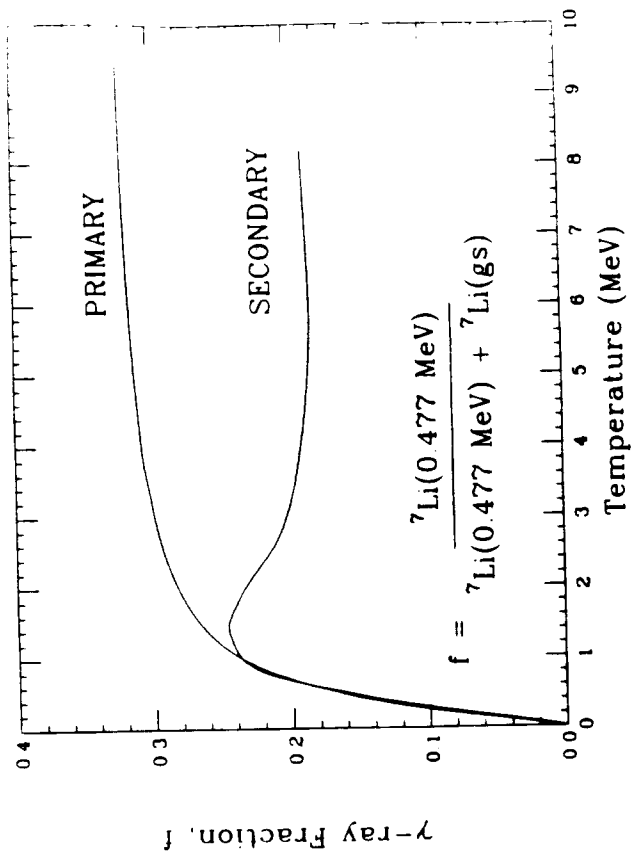


Figure 4 The variation of the fraction of ^7Li nuclei in the excited state as a function of the temperature (44). The predicted effect of sequential decay on the population ratio is shown by the curve labeled "SECONDARY" (44, 52).

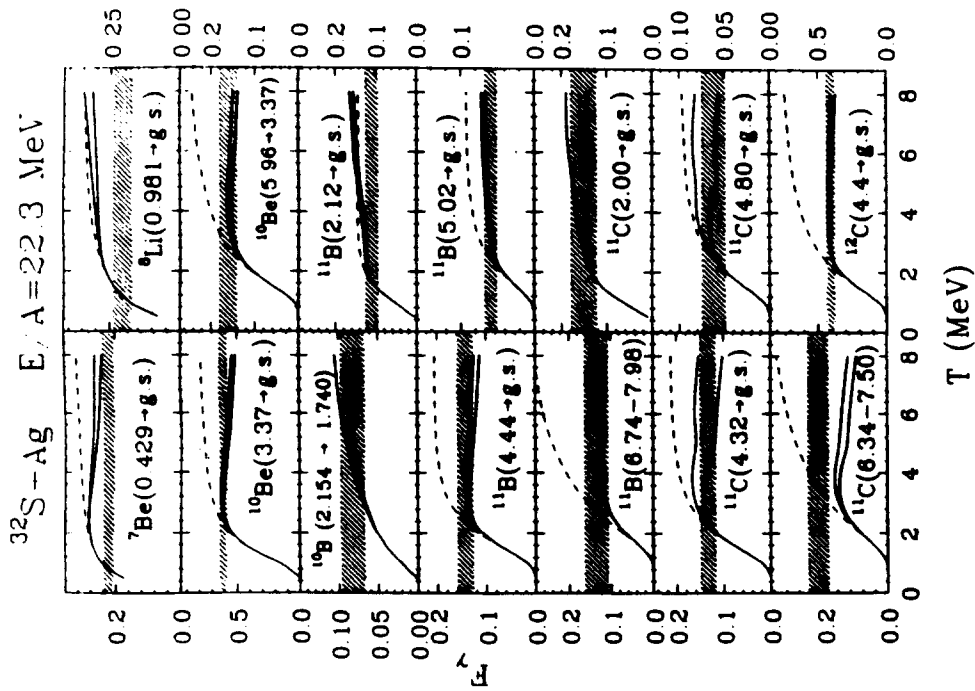


Figure 5 The γ -ray fractions for fragments in the range of $7 \leq A \leq 12$ from the reaction of $^{32}\text{S} + \text{Ag}$ at $E/A = 22.3$ MeV are shown by the cross-hatched areas. (63). The energies of the states are indicated in the panels. The range of the predicted fractions after sequential decay are shown by the solid lines. The dashed lines indicate the fractions calculated with sequential decay without feeding from

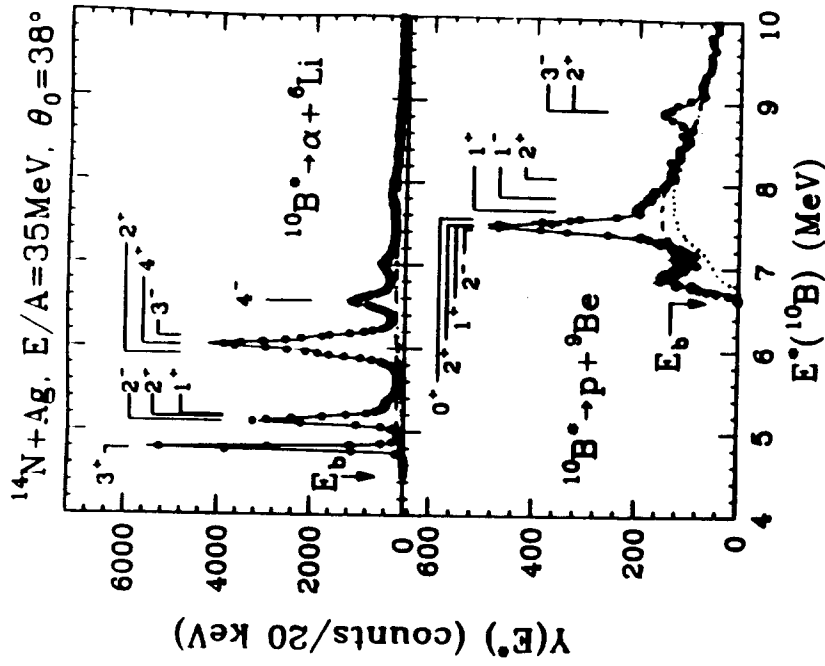


Figure 6 The measured excitation energy spectrum for the decay of ^{10}B into the $\alpha + {}^6\text{Li}$ channel, top, and the $p + {}^9\text{Be}$ channel, bottom from (46)

$^{36}\text{Ar} + ^{197}\text{Au}$, $E/A=35\text{MeV}$, $\theta_{av}=39^\circ$

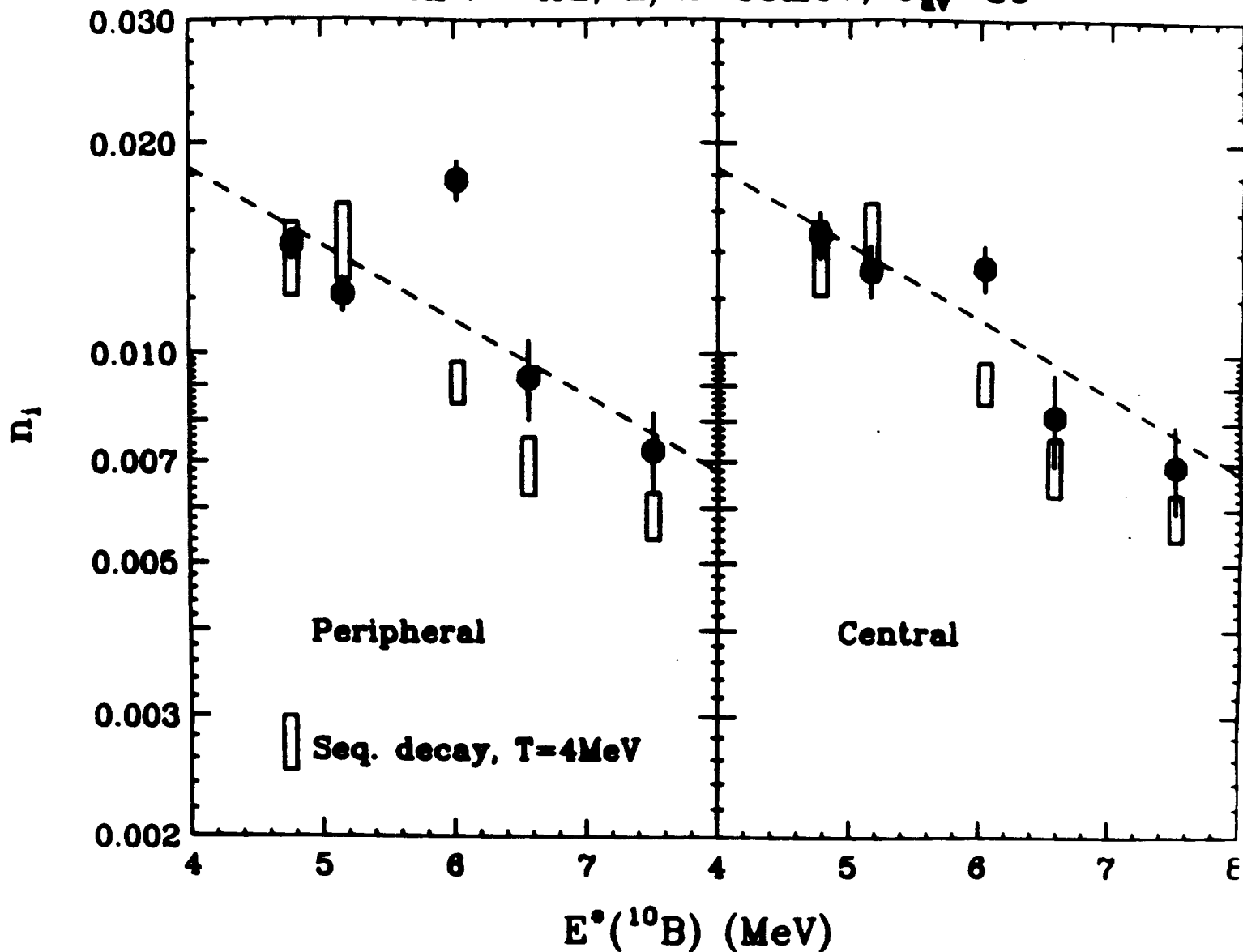


Figure 7 The relative populations of states in ^{10}B , normalized by the spin-degeneracy, are shown as a function of their excitation energy with central and peripheral collision triggers (78). The predicted yields including sequential decay are shown by the open boxes, and a simple exponential with $T=4$ MeV is shown by the dashed line.

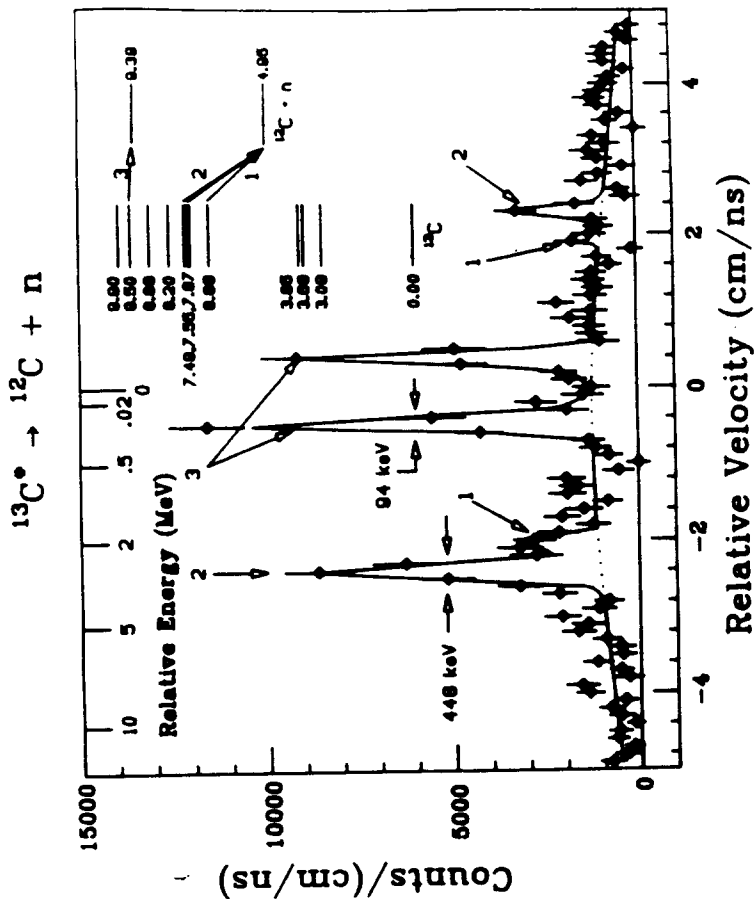


Figure 9 The relative velocity of colinear neutrons and ^{12}C residues from (85). The numbered peaks correspond to the transitions indicated in the inset level diagram. The solid line was fit to the data based on the known geometry, the energies of the states and the detector efficiency.

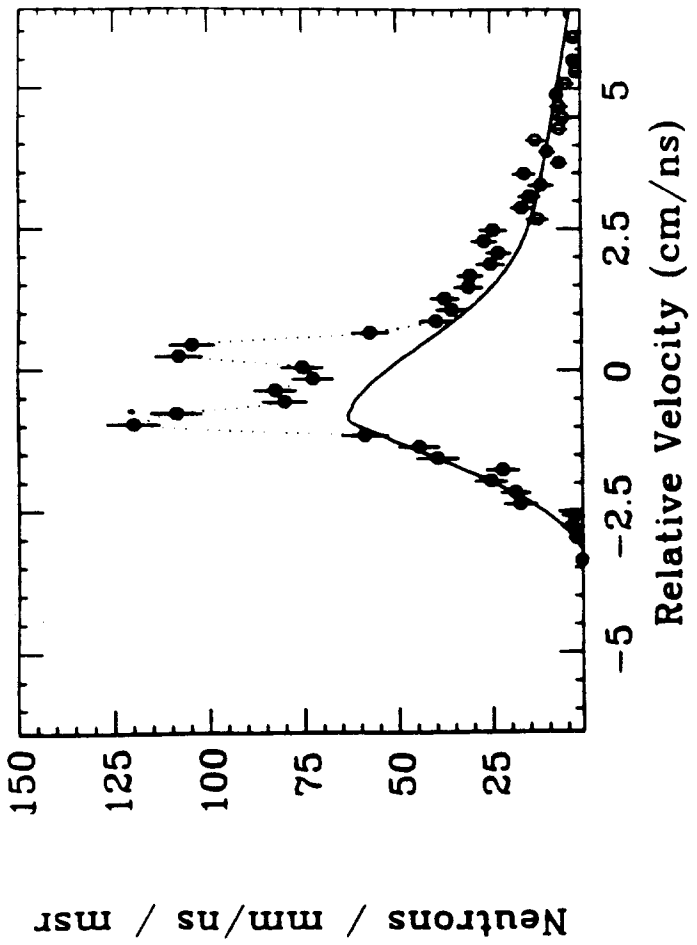


Figure 8 The yield of colinear neutrons in coincidence with ^7Li fragments as a function of the relative velocity of the two particles (83). The solid line indicates the contribution from the thermal background. The two peaks are created by the forward and backward going decay of a single state.

